

# Inhibition of bacterial growth by antibiotics: a minimal model

Ledoux Barnabé<sup>1,\*</sup>, Lacoste David<sup>1</sup>

**1** Gulliver Laboratory, UMR CNRS 7083, PSL Research University, ESPCI, Paris  
F-75231, France

\* barnabeledoux@gmail.com

## Abstract

Growth in bacterial populations generally depends on the environment (availability and quality of nutrients, presence of a toxic inhibitor, product inhibition..). Here, we build a minimal model to describe the action of a bacteriostatic antibiotic, assuming that this drug inhibits an essential autocatalytic cycle of the cell metabolism. The model recovers known growth laws, can describe various types of antibiotics and confirms the existence of two distinct regimes of growth-dependent susceptibility, previously identified only for ribosome targeting antibiotics. We introduce a proxy for cell risk, which proves useful to compare the effects of various types of antibiotics. We also develop extensions of our model to describe the effect of combining two antibiotics targeting two different autocatalytic cycles or a regime where cell growth is inhibited by a waste product.

## Introduction

The emergence of antibiotic resistance, which often occurs under changing levels of antibiotics is a major concern for human health [1, 2]. In an important class of antibiotics, called bacteriostatic antibiotics [3], the drug does not induce death directly, but renders some essential process in the cell metabolism less efficient or inactive [4–9] resulting in a reduced cell growth. For these antibiotics, it is essential to properly model cell metabolism and cell growth in order to better understand the action of antibiotics [10–13]. According to [14], the distinction between bacteriostatic and bactericidal antibiotics that target ribosomes depends on the value of their dissociation rate from the ribosomes. Antibiotics with slow dissociation rates are more likely to induce cell death and be classified instead as bactericidal because of the depletion of essential proteins they cause.

In the field of bacterial growth, the study of growth laws [15–17] represents a major step forward in our understanding of cell growth. These growth laws result from conservation of ribosome capacity and flux balance at steady-state. Recently, a new way to understand them has been put forward, that relies on a description of the cell metabolism as an ensemble of autocatalytic cycles, such as the cycle of ribosome production and that of RNA polymerase production [18]. By definition, an autocatalytic cycle implies a set of reactions and a set of species, so that all species of the set can be produced in increasing number by running the autocatalytic cycle [19]. The method, which we apply in this paper, has wide applications for addressing various questions related to cell growth [20]. For instance, it has been recently used to formulate predictions about the interplay between cellular growth rate and mRNA abundances [21].

While some predictions about the action of RNA-polymerase targeting antibiotics have been derived in Ref. [18], the full consequences for the inhibition of growth by a general antibiotics have not. In particular, this work does not discuss the second growth law that describes the inhibition of translation by antibiotics, nor the possibility that there may be two different regimes for the action of antibiotics, namely the so-called reversible and irreversible binding regimes of antibiotics. This distinction is quite important in practice because for reversible binding, faster growth in the absence of the drug leads to an increased susceptibility, while the opposite is true for irreversible binding [13]. Further, a regime of antibiotics concentration exists where two values of growth rate are possible (growth rate heterogeneity or bistability [22]) for the same range of physical parameters. A recent study of a wide class of antibiotics reported that this growth rate heterogeneity is variable depending on the target molecules [23], but at the moment, it is not clear how to model or predict this growth rate heterogeneity.

To summarize, we believe that the inhibition of bacterial growth by antibiotics has not been considered from a sufficiently general point of view, which motivates the present study. By building on Refs. [18] and [13, 24], we develop a general framework for the inhibition of bacterial growth by bacteriostatic antibiotics in which the cell metabolism is modeled as coupled autocatalytic cycles. Our work applies to all antibiotics for which the target molecule is an intermediate in an autocatalytic cycle of the cell metabolism that couples to cell growth, leaving aside other types of antibiotics that may for instance kill the cell without affecting its growth. Given the central role played by Ref. [13, 24] in our work, we start by a quick summary of the main findings of this paper. In the next section, we present our model, so that the new elements which we have introduced appear clearly. Then, we explore some consequences, concerning growth laws, and we test our model with experimental data on the dependence of the growth rate as function of the concentration of antibiotics for a wide range of different antibiotics. Then, we introduce a new proxy of cell risk induced by the antibiotics and we present some extensions of our model for more complex situations involving the combined action of multiple antibiotics [25–27] or the indirect effect due to the accumulation of a product with inhibition properties.

## Model for the inhibition of bacterial growth by antibiotics

Here, we recapitulate the main findings of a classic model of inhibition of bacterial growth by antibiotics [13], which is applicable to antibiotics that target ribosomes. In this model, the cell is viewed as a compartment in which the antibiotic present outside the cell can enter and bind to ribosomes. The perturbation of translation produced by the antibiotics is described by growth laws, which quantify the interdependence of the cell growth rate  $\lambda$  with the intracellular ribosome concentration  $r$ . The first law states that the ribosome concentration should increase linearly with the growth rate according to [15–17]:

$$r_u = r_{min} + \frac{\lambda}{\kappa_t}, \quad (1)$$

where  $\kappa_t$ ,  $r_u$  and  $r_{min}$  are respectively the translation capacity, the concentration of unperturbed ribosomes and a minimal ribosome concentration.

The second growth law states that, in the presence of an antibiotic inhibiting translation, the ribosome production is up-regulated, which also leads to another linear relation

$$r_{tot} = r_u + r_b = r_{max} - \lambda \Delta r \left( \frac{1}{\lambda_0} - \frac{1}{\kappa_t \Delta r} \right), \quad (2)$$

where where  $r_b$  is the concentration of ribosomes bound to the antibiotics and  
 $\Delta r = r_{max} - r_{min}$  is the dynamic range of the ribosome concentration. In other words,  
the second growth law describes the increased production of ribosomes that follows  
translation inhibition. As a result, the total ribosome concentration becomes negatively  
correlated with the bacterial growth rate in the presence of these inhibitors.

Now the antibiotics enter the cell and bind to the ribosomes, with the rate  
 $f(r_u, r_b, a) = -k_{on}a(r_u - r_{min}) + k_{off}r_b$  where  $k_{off}$  and  $k_{on}$  are first and second order  
rate constants and  $a$  is the antibiotic concentration inside the cell. Antibiotics can only  
bind to ribosomes if their concentration is above the minimum threshold  $r_{min}$  according  
to this formula. The flux of antibiotic concentration into the cell is  
 $J(a_{ex}, a) = P_{in}a_{ex} - P_{out}a$ , where  $a_{ext}$  is the antibiotic concentration outside the cell.  
Antibiotics enter the cell with rate  $P_{in}$  and exit with rate  $P_{out}$ , which could occur due  
to diffusion by passive transport or through pores by active transport [28, 29].

Together, these assumptions lead to the following dynamical equations [13]:

$$\begin{aligned}\frac{da}{dt} &= -\lambda a + f(r_u, r_b, a) + J(a_{ex}, a), \\ \frac{dr_u}{dt} &= -\lambda r_u + f(r_u, r_b, a) + s(\lambda), \\ \frac{dr_b}{dt} &= -\lambda r_b - f(r_u, r_b, a),\end{aligned}\quad (3)$$

where  $s(\lambda) = \lambda r_{tot}$  represents the ribosome synthesis rate.

In the absence of inhibitors, the pre-exposure or basal growth rate is  $\lambda_0$ , which  
corresponds to the normal behavior of the cell. The steady-state solution of this model  
is given by the following cubic equation [13]:

$$0 = \left(\frac{\lambda}{\lambda_0}\right)^3 - \left(\frac{\lambda}{\lambda_0}\right)^2 + \frac{\lambda}{\lambda_0} \left[ \frac{1}{4} \left(\frac{\lambda_0^*}{\lambda_0}\right)^2 + \frac{a_{ex}}{2IC_{50}^*} \frac{\lambda_0^*}{\lambda_0} \right] - \frac{1}{4} \left(\frac{\lambda_0^*}{\lambda_0}\right)^2. \quad (4)$$

The reversibility of the binding of the antibiotic is characterized by the parameter  
 $\lambda_0^* = 2\sqrt{P_{out}K_D\kappa_t}$ ,  $K_D$  is the dissociation constant  $k_{off}/k_{on}$  and  $IC_{50}^*$  is a typical  
concentration such that  $IC_{50}^* = \Delta r \lambda_0^*/2P_{in}$ . Since Eq. 4 is a cubic equation in the  
growth rate, there are one or three solutions, and in particular there is a parameter  
regime in which the dynamical system can be multi-valued.

The model predicts two regimes depending on the value of  $\lambda_0^*$ , called the reversible  
and irreversible limits. The reversible limit  $\lambda \ll \lambda_0^*$  describes a regime of strong outflux  
of toxic agents and unbinding rate. In that case, the growth rate has a smooth behavior  
described by:

$$\frac{\lambda}{\lambda_0} = \frac{1}{1 + \frac{a_{ex}}{IC_{50}}} \quad (5)$$

This smooth behavior is due physically to a rapid equilibrium which is reached between  
intra and extra cellular antibiotic pools.

In contrast, the irreversible limit  $\lambda \gg \lambda_0^*$  corresponds to negligible outflux and  
unbinding rate compared to the influx of toxic agents and binding rate. In that case,  
one obtains a discontinuous function:

$$\lambda = \frac{\lambda_0}{2} \left( 1 + \sqrt{1 - \frac{4P_{in}a_{ex}}{\Delta r \lambda_0}} \right). \quad (6)$$

In this regime, the system behaves as a toggle switch behavior, due to the competition  
between the antibiotic influx and the ribosome production.

By analyzing various types of antibiotics, the authors of [13] found that experimental  
data for bacteriostatic antibiotics indeed fit into one class or the other. Another major

insight of the model, was the prediction of different growth dependent susceptibility for the two classes of antibiotic behaviors. This susceptibility is measured thanks to the half-inhibition concentration  $IC_{50}$ , which is defined as the concentration of toxic agent at which the growth rate is half its initial value. This is a measure of the sensitivity of the system to external stress, the higher it is, the more resistant is the system to inhibitors. By substituting  $a_{ex} = IC_{50}$  and  $\lambda = \lambda_0/2$  into Eq. 4, one finds that the half inhibitory concentration  $IC_{50}$  falls onto a universal growth dependent susceptibility curve:

$$\frac{IC_{50}}{IC_{50}^*} \simeq \frac{1}{2} \left( \frac{\lambda_0^*}{\lambda_0} + \frac{\lambda_0}{\lambda_0^*} \right). \quad (7)$$

## Modified model based on autocatalytic cycles

We now introduce our model for cell metabolism as two coupled autocatalytic cycles, in which one cycle describes the production of ribosomes, while the other describes RNA-polymerase production [18]. These two autocatalytic cycles are coupled because ribosomes are necessary to synthesize RNA-polymerase protein subunits and vice-versa for ribosomes:  $B_1$  represents the number of active ribosomes;  $C_1$  the number of active RNA polymerases; similarly  $B_2, \dots, B_{N-1}$  and  $C_2, \dots, C_{K-1}$  are the abundances of intermediates involved in the assembly of ribosomes and RNA polymerases respectively,  $B_N$ ;  $C_K$  are the abundances of fully assembled but resting ribosomes/RNA polymerases respectively. Similarly to the classic model we first presented, we suppose that "toxic" inhibiting agents in numbers  $A$  can bind to one of the autocatalysts (chosen here to be  $B_1$  for simplicity) with a rate  $k_{on}$  and unbind with a rate  $k_{off}$ , proportionally to the relative abundance of antibiotics in the cell [13]. We denote  $B_{1,u}$  the abundance of unbound ribosomes and  $B_{1,b}$  the abundance of bound ribosomes.

The signification of the different variables in the model is summarized in the table 1.

$B_{1u}$	Number of fully formed free active ribosomes
$B_{1b}$	Number of fully formed ribosomes bound to antibiotics
$A$	Number of toxic agent molecules within the cell
$a_{ex}$	Concentration of toxic agent molecules outside the cell
$\Omega$	Cell volume
$B_k$ for $k \geq 2$	Number of ribosomes precursors
$C_1$	Number of fully formed and active RNA-polymerases
$C_k$ for $k \geq 2$	Number of RNA-polymerase precursors
$N$ (resp. $K$ )	Number of building steps for ribosomes (resp. RNA-polymerase)

**Table 1.** Variables of the model. Note that we used dimensionless numbers for species within the cell, except for  $a_{ex}$  which has the unit of a concentration and  $\Omega$  which has the unit of a volume.

In our model, we rely on Leontief's production function [19, 30] (see Appendix Section E for details), according to which the rates of reactions involving two complementary resources are set by the limiting quantity among the two using a minimum function. Historically, this law of the minimum has been introduced by Leontief's in his work in economy [31]: in a network of firms producing one product each by consuming the outputs of other firms (resources), the rate of production will be set by the availability of the scarcer resource. A similar idea was developed later by Liebig in ecology [32]. More recently, it was used for modeling autocatalytic cycles in metabolism [18]. With this method, we get linear equations in regimes where one reactant is scarce. This is similar to assuming that one reactant is in excess in a chemical reaction, and that the kinetics is set by the concentration of the scarcer reactant.

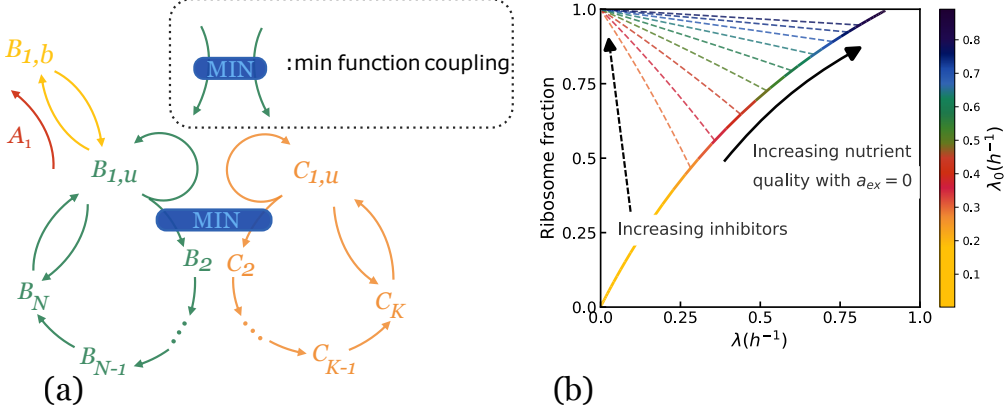


**Fig 1.** (a) Scheme of coupled autocatalytic networks interacting with a toxic agent. The blue box linking two arrows represents a coupling through a min function [31, 32]. (b) The first growth law is the increase of the ribosome fraction with the growth rate (solid curve), the second growth law corresponds to the dashed colored lines obtained by varying the amount of antibiotics. The pre-exposure growth rate  $\lambda_0$  displayed on the right scale.

Unlike in the previous model, which was formulated in terms of concentrations, our approach uses abundances or numbers [33] precisely because it is based on the Leontief framework. Due to this difference, our dynamical equations formulated in terms of species numbers do not contain the growth rate explicitly unlike Eq. 3. Naturally, it is straightforward to show that the two formulations are equivalent, because of the assumption of balanced growth for the cell. In this regime, all species present in the autocatalytic cycles grow at the same rate  $\lambda = d \ln \mathcal{N} / dt$ , where  $\mathcal{N}$  is typically the number of ribosomes or RNA-polymerases... Note that the cell volume is not constant but also grows at the same rate as the abundances of species inside the cell. This is the reason for the use of fractions defined with respect to the total abundances of mature molecules  $B_{tot} = B_{1,u} + B_{1,b} + B_N$ .

One can then combine the equations of the model to obtain a linear matrix equation for the sub-populations of ribosomes only, without explicit dependence on antibiotics, and a self consistent equation for the growth rate  $\lambda$  of the whole cycle (see Appendix, section A). In the following, we assume the cycle targeted by the toxic agent becomes limiting. The effect of the inhibition of one cycle on the other cycle is only considered in Appendix, section C.2. Consequently, we isolate the inhibited cycle and study its growth, because it restricts the growth of the rest of the network.

## Growth laws

A key quantity is the fraction of active ribosomes  $Q(\lambda) = B_{1,u}/B_{tot}$ , which takes the form of a polynomial in terms of the cell growth rate  $\lambda$  with factors depending on the rate constants  $k_{B,i}$  of reaction steps of the autocatalytic cycle :

$$Q(\lambda) = \frac{1}{k_{B,1}} \left( 1 + \frac{\lambda}{k_{B,2}} \right) \times \dots \times \left( 1 + \frac{\lambda}{k_{B,N-1}} \right) \left( \lambda + \frac{1}{\tau_{life}} \right), \quad (8)$$

where  $\tau_{life}$  is the life time of mature intermediates  $B_N$ ,  $B_{1,u}$  and  $B_{1,b}$ , which corresponds to the time of degradation of these molecules. This life time is assumed to be of the same order for all these species for simplicity and is typically large in comparison with the growth rate, unless the cell is in a regime of reduced growth [21].

The expression above simplifies to  $Q(\lambda) \simeq \lambda/k_{B1}$  in the limit of "fast assembly" 166  
 $k_{B,2}, \dots, k_{B,N-1} \gg \lambda$  and long ribosome lifetime  $\lambda \gg 1/\tau_{life}$ . In this case, the results do 167  
not depend on the number of steps  $N$  in the first cycle. We also understand from Eq. 8 168  
that if one step  $n$  becomes limiting, the term  $\lambda/k_{B,n}$  cannot be ignored, which modifies 169  
 $Q(\lambda)$ . With the above conditions, we recover the linear increase of the fraction of 170  
unbound ribosomes with respect to  $\lambda$ , which is the *first growth law*: 171

$$\frac{B_{1,u}}{B_{tot}} \simeq \frac{\lambda}{k_{B,1}} + \frac{1}{k_{B,1}\tau_{life}}. \quad (9)$$

Note that this is the equivalent of Eq. 1 in the previous model. This law describes the 172  
increase of the fraction of unbound ribosomes with the growth rate under changes of 173  
nutrient quality in the absence of antibiotics, so when  $a_{ex} = 0$ . Here, increasing the 174  
nutrient quality can be realized by increasing assembly rates  $k_{B,2}, \dots, k_{B,N-1}$ , assuming 175  
that they are equal to each other. Indeed, if only one of these rates were increased, the 176  
other steps would be limiting and we would not see the effect we are interested in. In 177  
the end, we obtain the solid blue curve in Fig. 1b, which approaches the origin when 178  
 $\lambda$  goes to zero due to the long lifetime assumption. 179

When an antibiotic inhibiting translation is present, the ribosome fraction 180  
 $(B_{1,u} + B_{1,b})/B_{tot}$  decreases with the growth rate, which is the *second growth law* [15]. 181  
With our formalism, we indeed obtain a negative correlation between these variables, 182  
which takes a linear form: 183

$$\frac{B_{1,u} + B_{1,b}}{B_{tot}} \simeq 1 - \frac{\lambda}{k_{B,3}}, \quad (10)$$

if we assume fast assembly, fast activation, long ribosome lifetime  $\lambda \gg 1/\tau_{life}$  and a 184  
single intermediate step ( $N = 3$ ). This equation is the equivalent of the second growth 185  
law described by Eq. 2. Without specific assumptions on the rates, one obtains the 186  
colored curves in Fig. 1b, which have been obtained by varying the external 187  
concentration of antibiotics  $a_{ex}$  keeping all other parameters fixed. 188

As the concentration of antibiotics increases, the growth rate always decreases below 189  
the basal growth rate  $\lambda_0$ . We find that for  $a_{ex} = 0$ , the decreasing and increasing curves 190  
of Fig. 1b cross each other, which is expected because  $\lambda = \lambda_0$  at this point. 191

It is important to appreciate that the first and the second growth laws are derived 192  
from our model, while they were introduced as phenomenological constraints in Eq. 1 193  
and Eq. 2 in the model we first presented. Further, in the original work on growth 194  
laws [17], linear dependencies with respect to the growth rate were reported. In contrast 195  
to this, we see from Fig. 1, that neither the first nor the second growth law is strictly 196  
described by linear relations. A small curvature is indeed visible for the curves that 197  
correspond to the second growth law (when the translation is inhibited by an antibiotic) 198  
in the experimental data of [17], which is reported in Fig 5 of Ref. [34], yet the few 199  
experimental points make it complicated to assess this effect clearly. It is difficult to 200  
appraise whether there is a curvature for the first growth law in this data, because there 201  
is not enough data available in the low growth rate region. 202

We now explore further consequences of our formalism. Let us first consider the case 203  
of arbitrary number of intermediates ( $N$ ), for which we have obtained the self-consistent 204  
equation for  $Q(\lambda)$  given in Eq. 34. 205

The reversible limit  $\lambda \ll \lambda_0^*$  describes a regime of strong outflux of toxic agents and 206  
unbinding rate. We find that in this limit (see Appendix, section A): 207

$$Q(\lambda) = \frac{1}{1 + \frac{K_D P_{in}}{P_{out}} a_{ex}}. \quad (11)$$

In contrast, the irreversible limit  $\lambda \gg \lambda_0^*$  corresponds to negligible outflux and 208  
unbinding rate compared to the influx of toxic agents and binding rate. Then, we 209

obtain a different equation setting the growth rate (see Appendix, section A):

$$Q(\lambda) = 1 + \frac{P_{in}a_{ex}}{\lambda}. \quad (12)$$

For ribosomes in the regime of intermediate or high growth rates, we can expect a long lifetime, a small resting rate, fast assembly and fast activation [18]. These conditions translate to  $\frac{1}{\tau_{life}}, k_{B4} \ll \lambda_0, k_{B1} \ll k_{B2}, \dots, k_{B,N}$ , yielding  $\lambda_0 \simeq k_{B1}$ . In this limit, we can simplify our self-consistent equation for the growth rate

$$\frac{P_{in}a_{ex}}{\left( \frac{k_{B1}}{k_{on}} \frac{\lambda + P_{out}}{\lambda} + \frac{\lambda}{\lambda + k_{off}} \right)} \simeq \left( 1 - \frac{\lambda}{\lambda_0} \right) (\lambda + k_{off}), \quad (13)$$

so that we recover the equation derived in [13]. With the additional assumption of fast binding  $\lambda_0 \ll k_{on}$ , the possible values of the growth rate are roots of a polynomial, from which it is possible to recover the reversible and irreversible limits of antibiotics binding described previously. Further, we find in this limit  $Q \simeq \lambda/\lambda_0$ .

Interestingly, the self-consistent equation for the growth rate obtained within the autocatalytic framework (see Appendix, section A) has two solutions in the irreversible limit with fast assembly, leading to two separate branches of solutions for  $\lambda$ . A first solution remains close to 0, corresponding to a non-growing cell. A second one is larger but exists only until a given concentration of inhibitors is reached, above which the system jumps on the other branch, and the growth rate vanishes as shown in Fig. 4a. In experiments, in the irreversible case, the system usually starts from  $\lambda_0$  and the growth rate decreases as the concentration of inhibitors increases, until the discontinuity where the growth rate jumps on the second branch and vanishes. This growth rate heterogeneity happens above a threshold in terms of the antibiotic concentration. Such a phenomenon has been predicted in other theoretical works [13, 35], and it has also been observed experimentally [22, 36].

A very recent experimental study by M. Kals et al. (2025) quantified the growth heterogeneity (GRH) systematically for many antibiotics across different concentrations [23]. In this work, the growth rate heterogeneity is evaluated from the standard deviation of the growth rates at a given time point and averaged across multiple time points. The authors reported that this GRH typically increases near the minimum inhibitory concentration (MIC) and can be large or small depending on the type of antibiotics. In agreement with our predictions, they observed a small GRH for chloramphenicol and a large GRH for ampicillin or rifampicin for instance. One should note however, that in our model, the distinction between reversible or irreversible, which controls the GRH, is not purely a matter of the target molecule of the antibiotic. According to the definition of  $\lambda_0^*$ , the size of the efflux rate  $P_{out}$  matters also. This means that a molecule like tetracycline, which is expected to be reversible and to have a small GRH [23], can nevertheless display a coexistence between growing and non-growing states in some conditions as observed experimentally, when the duration of the drug exposure is short and in the presence of additional regulation mechanism that controls the efflux rate [37].

## Experimental test of the model

We have tested our model on a number of antibiotics, for which experimental data can be found in the literature [9, 13]: Chloramphenicol inhibits ribosome production by binding to ribosomes, preventing them from transcribing new proteins; Rifampicin targets RNA-polymerase by binding to RNA-polymerase [38, 39]; Kanamycin, Streptomycin, Chloramphenicol and Erythromycin target the ribosomal autocatalytic

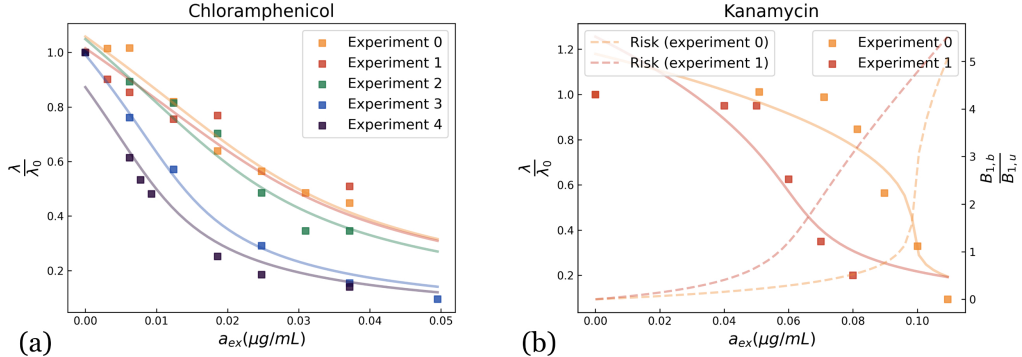


**Fig 2.** Comparison with experiments for two drugs affecting bacterial growth, namely (a) Chloramphenicol (data from [9] and [13]) and (b) Kanamycin (data from [13]). The solid line shows the growth rate as a function of the fraction of inhibitors, while the dotted line shows a measure of the risk faced by the cell defined in the text. The data were fitted by constraining the parameters as explained in Appendix. Different experiments for the same antibiotic correspond to different growth medium.

cycle [4, 6, 8, 40]; and finally Triclosan targets the synthesis of fatty acids [41–43], thus affecting the building of bacterial membranes [18]. In Fig.2, we show the normalized growth rate  $\lambda/\lambda_0$  as function of the concentration of antibiotics only for Chloramphenicol and Kanamycin, the plots for the other antibiotics are shown in Appendix, section B. The details of the fitting procedure, as well as the constraints and values imposed for the different parameters are explained and justified in Appendix Section B.2, where a table sums up these results.

In [18], the effects of Triclosan and Rifampicin were explained by adding Hill functions heuristically to describe saturation effects in the cycle. In contrast here, we provide an explicit expression for the dependence of the growth rate on the fraction of antibiotics without such an assumption. The fact that we are able to describe a large panel of antibiotics suggests that these antibiotics can indeed be depicted as inhibitors affecting essential cellular autocatalytic cycles despite their different mechanisms. Note that we recover different concavities in Fig.2, which correspond to the two distinct regimes of cellular response to the antibiotics previously identified for ribosome-targeting antibiotics [13]: the reversible limit where the outflux of antibiotics compensates the influx of the latter, and the irreversible limit where antibiotics bind quickly to autocatalysts, resulting in an accumulation of bound, inhibited individuals.

## Cell risk induced by the antibiotics

Antibiotics have a rather limited number of targets such as ribosomes [3, 4, 6, 10, 13] or RNA-polymerase [7] for instance. Regardless of the mechanism of action or precise targets, the effect of antibiotics on growth show similarities [12], which suggests that a general measure of the risk induced by the toxic agent might exist. In particular, bacteriocidal antibiotics do not appear to be fundamentally different from bacteriostatic ones, both reduce cell growth, but if the inhibition is too strong, processes that are necessary for survival cannot be satisfied and cell death can occur [10, 44]. In fact, it has been demonstrated that for ribosome targeting antibiotics, the cidality depends on the rate of dissociation of antibiotics (and thus on the amount of bound antibiotics in the cell) [14]. This study concluded that cell death induced by a ribosome targeting drug results from a prolonged inhibition of synthesis. This means that for sufficiently slow dissociation rates, antibiotics stay bound to ribosomes.

To quantify the effect of antibiotics, we introduce a measure of the risk faced by the cell, defined as the fraction of bound active individuals  $B_{1,b}$  (which could be for instance ribosomes or RNA polymerases or some of their intermediates) with respect to unbound active individuals  $B_{1,u}$ . The main interest of this definition is that it is independent of the type of action of the antibiotic and can be used to compare the efficiency of different antibiotics. It captures the inhibition of protein synthesis by the drug, which is also correlated to the cidalility of this drug [14]. A ratio smaller than 1 signifies that there are more active unbound ribosomes than bound ribosomes, thus setting a value above which the cell starts being significantly populated by bound ribosomes.

Naturally, other choices are possible for a proxy of cell risk. Relative growth suppression is certainly important too, but fails to capture the microscopic origin of the risk which is the point of the proposed definition. This proposed definition is also more explicit than  $B_{1,u}/B_{tot}$  (or  $B_{1,b}/B_{tot}$ ), which account for the fraction of active/inactive ribosomes in the pool rather than directly comparing bound ribosomes to unbound ones. Yet another possibility would be to compare the ratio of  $B_{1,u}$  in the presence and in the absence of antibiotics. A disadvantage of such a definition however is that it would require a choice of reference point for what low risk means and a characterization of that state.

Instead, with the proposed definition above, in terms of the fraction of active ribosomes, we have a direct link with a quantity that controls the production of proteins [8, 40]. Note that in the previous section, we analyzed Kanamycin, which is known to be bacteriocidal with the same framework we used for bacteriostatic antibiotics. This supports the idea of a proxy of cell risk applicable across various antibiotics types, at least in the early regime following the application of the drug where the reduction of growth is the main effect. We suspect that there might be a first threshold for this risk to enter a non-growing state and an higher one to enter the state of death. The distinction between the phenotypes of non-growth and death is that the cell can not recover from death but can recover from the non-growing state [45].

We show the prediction for this proxy of risk that follows from our model for the reversible and irreversible regimes in Fig.3.

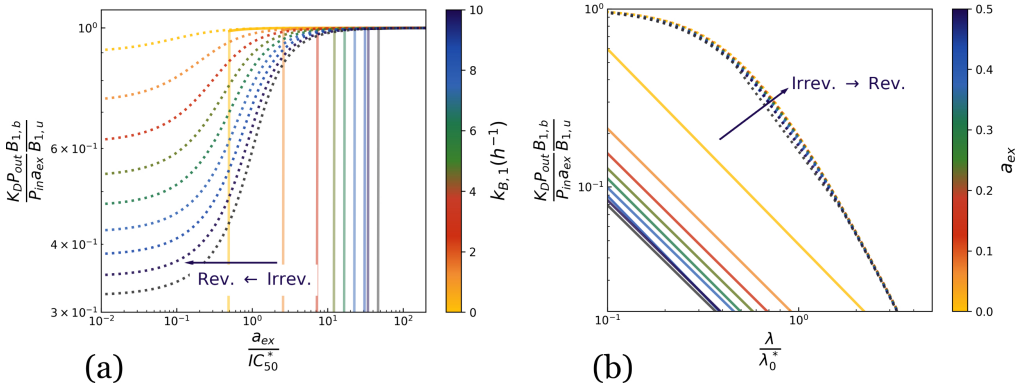


**Fig 3.** Normalized risk versus antibiotic concentration. (a) Risk faced by the system in the presence of a toxic agent. We compare the reversible case (dotted lines) and the irreversible case (full lines). (b) Rescaled risk depending on the growth rate. We compare the reversible case (dotted lines) and the irreversible case (full lines). We observe a complete collapse of the curves in the reversible limit. The risk is rescaled by  $\frac{P_{in} \alpha_{ex}}{K_D P_{out}}$ . The larger this ratio, the larger is the ability of antibiotics to enter the cell and bind to ribosomes, and the lower it is, the more antibiotics will unbind and exit the cell. Therefore this ratio correlates with bacterial cidalility.

284  
285  
286  
287  
288  
289  
290  
291  
292  
293  
294  
295  
296  
297  
298  
299  
300  
301  
302  
303  
304  
305  
306  
307  
308  
309  
310  
311  
312

This proxy of risk has a simple expression

314

$$\frac{B_{1,b}}{B_{1,u}} \simeq \frac{k_{B1}}{\lambda} - 1, \quad (14)$$

when ribosomes have a long lifetime, fast assembly and fast activation. Note that in Fig.3, the concentration of toxic agent is rescaled by a typical concentration inspired from [13],  $IC_{50}^* = \frac{\sqrt{K_D P_{out} k_{B,1}}}{P_{in}}$ .

As expected, the risk is increasing with the fraction of toxic agent while it is decreasing with  $\lambda_0$ . The risk increases rapidly close to  $IC_{50}^*$ , with a discontinuity at a given fraction  $a_{ex,lim}$  in the irreversible case. This fraction can be understood as a limit concentration above which the system is significantly endangered. In Fig.3, we rescale the risk by  $P_{in}a_{ex}/(K_D P_{out})$  to obtain a collapse of the experimental data in the reversible limit. Indeed for  $\lambda/\lambda_0^* \rightarrow 0$ , the risk is equivalent to  $P_{in}a_{ex}/(K_D P_{out})$  in the reversible limit which follows from Eq.14.

## Half-inhibitory concentration

Similarly to what was done in the first model presented, one can study the half-inhibitory concentration  $IC_{50}$  with a model based on autocatalytic cycles, assuming they contain an arbitrary number of steps  $N$  in the limit of long lifetime and fast assembly. If we can lump all intermediates into just one ( $N = 3$ ), we obtain

$$\frac{IC_{50}}{IC_{50}^*} = \frac{1}{2} \left( \left( \frac{\lambda_0^*}{\lambda_0} + 2K_D \frac{\lambda_0}{\lambda_0^*} \right) \left( 1 + \frac{\lambda_0}{2k_{off}} \right) + \frac{\lambda_0}{\lambda_0^*} \right), \quad (15)$$

where we have rescaled the half-inhibition concentration by a typical concentration  $IC_{50}^* = \sqrt{K_D P_{out} k_{B,1}}/P_{in}$  and the basal growth rate by  $\lambda_0^*$ . Note that this expression does not depend only on the ratio  $\lambda_0/\lambda_0^*$  but also on  $\lambda_0$  (itself defined by the parameters of the system). The rescaled half-inhibition concentration as a function of the rescaled basal growth rate in this limit is the convex function shown in Fig.4b. Remarkably, this function allows to collapse the measurements of many types of antibiotics in a way which is similar with what was done in Ref [13] (for this comparison the same experimental data has been used). Note also that in the limit of long lifetime, fast binding, fast assembly, and with  $k_{off} \gg \lambda_0$ , we recover the universal growth dependent susceptibility curve of Eq. 7.

For an arbitrary number of steps, we also recover in Fig.4b the two regimes of antibiotics binding mentioned before, namely the reversible regime where the half-inhibitory concentration decreases with  $\lambda_0$  and the irreversible regime where it increases with  $\lambda_0$ . Adding intermediate steps in the autocatalytic cycle shifts the minimum of the parabola towards lower  $\lambda_0$  and reduces  $IC_{50}$  and thus makes it easier to inhibit growth in the cycle. It also introduces a stronger dependence of  $IC_{50}$  on the rate constants  $k_{1,B}$  in the reversible regime as compared to the irreversible regime. This reflects that intermediate steps have a stronger impact in reversible pathways as compared to irreversible ones.

## Extensions of the model

Other phenomena can be treated with our framework, while we can not be exhaustive, we study two specific extensions: in the first one we consider the combined action of two antibiotics that target two coupled autocatalytic cycles and in the other one, we consider the possibility that the product of one cycle inhibits that cycle.

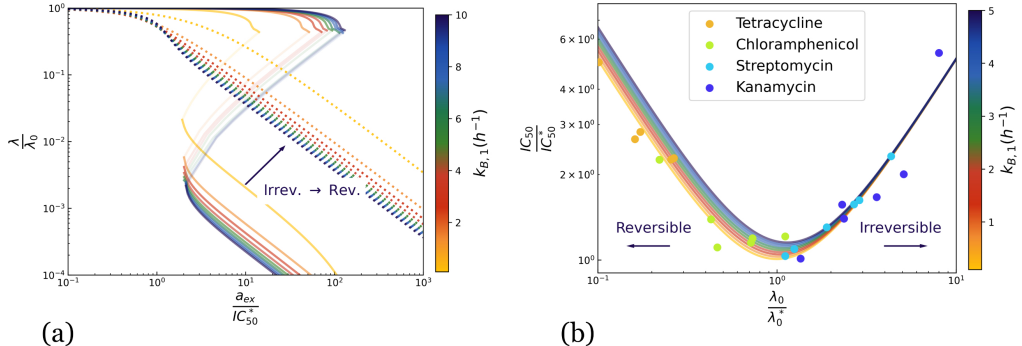


**Fig 4.** (a) Normalized growth rate versus the normalized antibiotic concentration. In dotted lines we represent the reversible regime  $k_{off}, P_{out} \geq k_{on}, P_{in}$ , in full lines the irreversible regime  $k_{off}, P_{out} \ll k_{on}, P_{in}$ . For the irreversible case (full lines), we observe two branches that represent the coexistence of two values of the growth rate, a "large" growth rate and a "near-zero" growth rate. A discontinuity appears when the system jumps from one branch to another. The colors of the curves correspond to different choices of rate constant  $k_{B,1}$  as shown on the scale on the right.  $k_{B,1}$  essentially sets the basal growth rate  $\lambda_0$  (see Appendix) and may vary from one cell to another in a population [46].  
(b) Half-inhibition concentration  $IC_{50}$  as function of the normalized pre-exposure growth rate. Symbols represent experimental data points extracted from Ref. [13], which correspond to various antibiotics as shown in the legend.

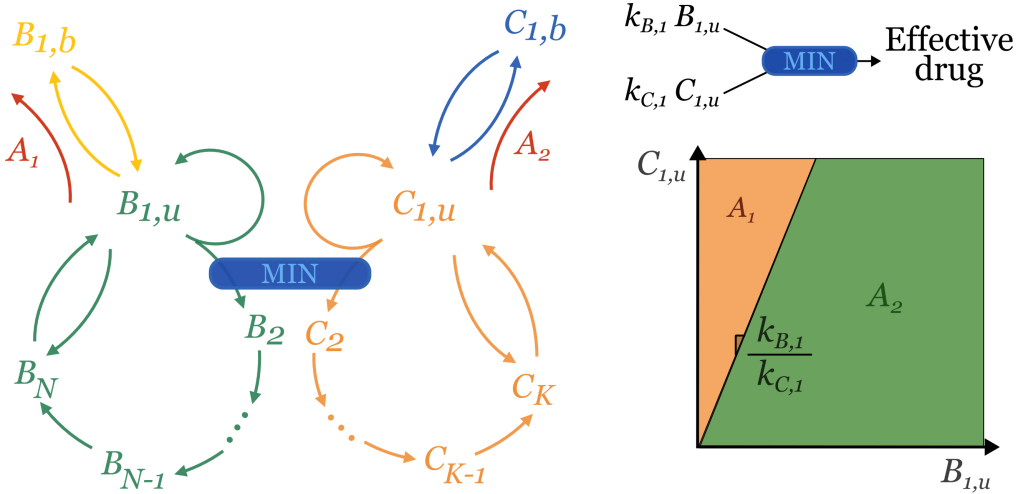
## Effect of two antibiotics targeting two coupled autocatalytic cycles

The combined action of two antibiotics targeting simultaneously the same ribosomes (and thus the same autocatalytic cycle) has been studied theoretically in [25] and experimentally validated in [26]. Interestingly, the authors found different regimes of drug interactions such as synergy (the combined effect is stronger) and antagonism (the combined effect is weaker). Another possibility is that the combined effects of the two drugs can be less than that expected based on the individual effect of the drugs, in which case one speaks of suppressive effects [27]. Inspired by these works, we now apply our framework to study the effect of two antibiotics  $A_1$  and  $A_2$  targeting molecules belonging to separate but coupled autocatalytic cycles as sketched in Fig.5. To be clear the type of combination of drugs we are interested here is for instance the case where the first drug targets ribosomes (like tetracycline) and the second one targets RNA-polymerase (like rifampicin) or DNA replication (like ciprofloxacin).

Interactions effects between two drugs can be quantified by the dose response surface, which represents the growth rate as function of both drug concentrations as shown in Fig.6. In the case we consider, the two autocatalytic cycles are coupled with a minimum function introduced previously. As a result, no synergy of the antibiotics is possible because the system behaves as if only one antibiotic was active for a given set of  $(a_{ex,1}, a_{ex,2})$ . Thus, we predict an *antagonistic* [25] interaction. In the literature, antagonistic interaction has indeed been observed with the combination of a first drug that targets ribosomes (like tetracycline) and a second one that targets DNA-synthesis (like ciprofloxacin) in agreement with our model [2]. In practice, the interaction becomes suppressive at higher concentration of ciprofloxacin, but that regime is not accessible from our approach.

On Fig.6, we also see that the transition from one drug to the other depends on the regime of action of each drug. On Fig.6a, drug 1 operates in the reversible regime

354  
355  
356  
357  
358  
359  
360  
361  
362  
363  
364  
365  
366  
367  
368  
369  
370  
371  
372  
373  
374  
375  
376  
377  
378  
379  
380



(a)

(b)

**Fig 5.** (a) Two antibiotics  $A_1$  and  $A_2$  targeting two different but coupled autocatalytic cycles (coupled through a min function represented with the blue box). (b) Predominance diagram of the two drugs, when  $B_{1,u}$  (resp.  $C_{1,u}$ ) gets small, the associated cycle is limiting and the effective antibiotic is the one targeting this cycle.

whereas drug 2 operates in the irreversible regime. If we fix  $a_{ex,1}$  (resp.  $a_{ex,2}$ ) and increase  $a_{ex,2}$  (resp.  $a_{ex,1}$ ), the growth rate will be constant until  $a_{ex,2}$  (resp.  $a_{ex,1}$ ) becomes large enough for drug 2 (resp. drug 1) to be the inhibiting drug, and it will start decreasing. We also observe that at fixed  $a_{ex,1}$ , the growth rate decreases more slowly with  $a_{ex,2}$  than it does with  $a_{ex,1}$  at fixed  $a_{ex,2}$ .

When the parameters are the same for the two drugs, the transition between the domains of predominance of each antibiotic is along the diagonal  $a_{ex,1} = a_{ex,2}$ . On Fig.6a, this transition is shifted upward as compared to Fig.6b where the two drugs are both reversible with the same parameters. Indeed on Fig.6a, as drug 1 produces a stronger inhibition than drug 2 at the same concentration, drug 1 is effective even in regions where  $a_{ex,1} < a_{ex,2}$ .

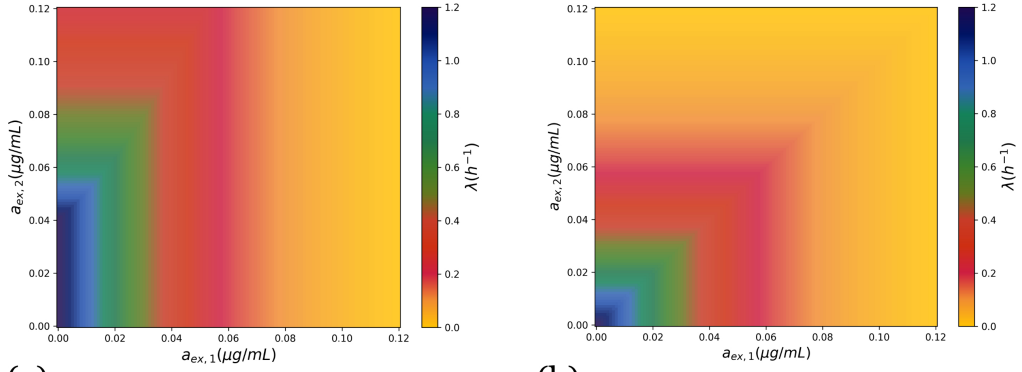
As shown in calculations detailed in Appendix Section C, the minimum law sets a transition between the effect of one antibiotic and the effect of the other one, depending on which cycle becomes limiting (when  $a_{ex,1} \gg a_{ex,2}$ , the cycle inhibited by  $a_{ex,2}$  becomes limiting and vice versa). Actually, the transition does not occur at  $a_{ex,1} = a_{ex,2}$  but when both terms of the minimum function shown in the Fig. 5 are identical.

## Closed compartment and inhibiting waste

In this section we show that our model can describe other systems than cycles inhibited by antibiotics. In particular we consider the network represented on Fig.7, in which a waste  $W$  is produced at a rate  $k_w$  (see Appendix Section C). This waste then inhibits autocatalysts by binding to them in a similar fashion than antibiotics in the previous sections. We consider only a closed compartment  $P_{in} = P_{out} = 0$ , meaning that waste only comes from the cycle itself and never leaves the compartment, then the risk is

$$\frac{B_{1,b}}{B_{1,u}} = \frac{k_{on}k_w Q(\lambda)}{(\lambda + k_{off})(\lambda + k_{on}Q(\lambda)\frac{\lambda}{\lambda + k_{off}})}, \quad (16)$$

where  $Q(\lambda)$  was defined in Eq.8. Interestingly, there are regimes where the risk is an



(a)

(b)

**Fig 6.** Dose response surface of two antibiotics targeting two coupled autocatalytic cycles. On (a), the drug 1 is in the *reversible regime* with parameters:  $P_{in(B)} = 40mL.\mu g.h^{-1}$ ,  $P_{out(B)} = 30h^{-1}$ ,  $k_{B,1} = 2h^{-1}$ ,  $\tau_{life(B)} = 10^2h$ , while drug 2 is in the *irreversible regime* with parameters:  $P_{in(C)} = 0, 7mL.\mu g.h^{-1}$ ,  $P_{out(C)} = 2h^{-1}$ ,  $k_{C,1} = 1h^{-1}$ ,  $\tau_{life(C)} = 10^2h$ . On (b) instead, both drugs are in the *reversible regime* with parameters  $P_{in} = 40mL.\mu g.h^{-1}$ ,  $P_{out} = 30h^{-1}$ ,  $k_{B,1} = k_{C,1} = 1h^{-1}$ ,  $\tau_{life(B)} = \tau_{life(C)} = 10^2h$ .

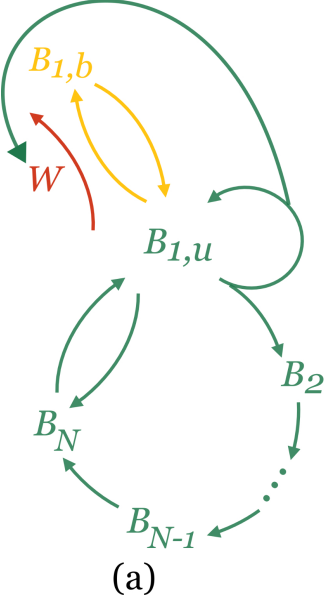
increasing function of the growth rate  $\lambda$  as shown on Fig.7. This regime corresponds to an accumulation of bound individuals when the growth rate is increasing, which are not diluted fast enough.

Some biological processes where the bacteria produces a self-inhibitory compound may be modeled in such a way, for instance the production of ribosome modulation factor [47] or inhibition due to by-products in yeast [48].

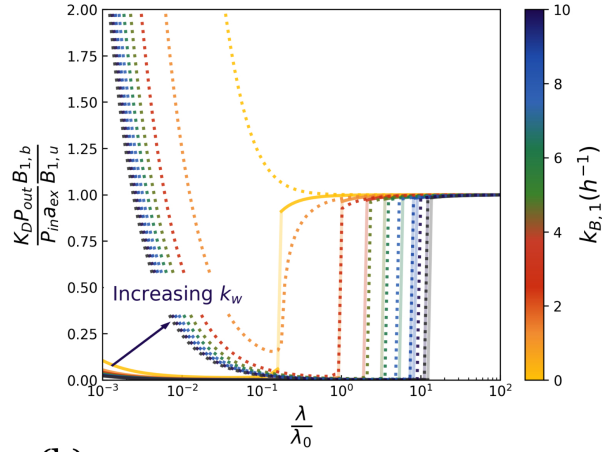
## Conclusion

We constructed a biophysical framework for the inhibition of bacterial growth by antibiotics based on the view that cell metabolism is based on coupled autocatalytic cycles. Unlike what was done in Ref. [13], our approach does not assume growth laws, instead they are derived from the model. The model describes well the effects of a large panel of antibiotics targeting key autocatalytic cycles in E.Coli. We have found that the two regimes previously identified for ribosome-targeting antibiotics in [13], namely the reversible (strong outflux of inhibitors) and irreversible (small outflux of inhibitors) regimes, should in fact be expected generically. Further, we found a region of growth rate heterogeneity in a certain range of parameters and for certain antibiotics, which has been reported experimentally. We were also able to describe the antagonistic effect of two drugs targeting different autocatalytic cycles, in the specific case where one drug targets ribosomes while the second drug targets the RNA-polymerase activity or the DNA synthesis.

In the future, we would like to expand our approach towards bacteriocidal antibiotics, which are typically used in conjunction with bacteriostatic antibiotics in a time-dependent manner [49]. The observation that our model successfully describes the effect of Kanamycin although this antibiotic is classified as bacteriocidal suggests that bacteriocidal antibiotics may also lower the growth rates similarly as bacteriostatic antibiotics before they kill the cell. This suggests that the frontier between these two classes of antibiotics is somewhat blurry, as also confirmed by the observation that this frontier depends on antibiotic concentration and on the duration of the drug exposure. In this context, we hope that the proxy of risk which we have introduced could be a



(a)



(b)

**Fig 7.** (a) Network where self inhibiting waste is produced. (b) Risk related to growth in a regime where risk can be increasing with  $\lambda$ . The full lines corresponds to a higher value of  $k_w$  ( $k_w = 0.01 h^{-1}$ ) compared to the dotted lines ( $k_w = 1 h^{-1}$ ).

useful measure to navigate between the three relevant phenotypes, namely that of a growing cell, a non-growing cell and a dead cell.

We are planning to also study experiments that show significant cell-to-cell heterogeneity in antibiotic susceptibility [36, 50]. Modeling these experiments will require a stochastic version of the present model which is needed for describing the growth and death of individual cells and the stochastic effects due to population size. In this respect, it is encouraging to see that our model predicts growth rate heterogeneity even in the absence of noise as seen experimentally, but more single-cell studies similar to [23], are needed to analyze this growth rate heterogeneity more precisely and to relate the single-cell behavior to population susceptibility.

We have also explored the question of drug interactions inspired by Ref. [25], which was also built on [13] and therefore also used *phenomenological growth laws* as assumptions. Since our model relied instead on a more detailed modeling of translation and transcription using autocatalytic cycles, we were able to study unexplored mechanism of action of antibiotics, such as the case where the two antibiotics target two coupled cycles, which could be ribosomal for the first cycle and m-RNA or DNA synthesis for the second one. In this case, we predict antagonist interactions among the two drugs and a dose response surface which depends whether the two drugs are in the same binding regime or in different ones. Antagonist interactions have indeed been reported in the case where the two drugs target ribosomes and DNA-synthesis.

Finally, let us also point out that our approach based on autocatalytic cycles is rather general and could be applied beyond cellular biology to other fields, such as ecology [51] or economy, where individuals rather than molecules are able to create more of themselves thanks to autocatalytic cycles but can also be inhibited by toxic agents, either present in their environment or created by themselves as a result of their own growth, a case we also considered in the last extension of this framework.

434  
435  
436  
437  
438  
439  
440  
441  
442  
443  
444  
445  
446  
447  
448  
449  
450  
451  
452  
453  
454  
455  
456  
457  
458  
459

## Acknowledgements

We acknowledge inspiring discussions with C. Baroud and E. Maikranz, and a critical reading by L. Dinis.

## A Definition of the model and derivation of the growth laws

The law of the minimum used here to model cell metabolism actually emerges from works in economy and are related to the Leontief's production function. This law concerns the formation of a product  $P$ , for which  $n_1$  units of  $R_1$ ,  $n_2$  units of  $R_2$ , ... up to  $n_N$  units of  $R_N$  are assembled. The production rate of  $P$  is limited by the smaller value of  $R_j/n_j$ , that is the number of sets of resource  $j$  required to produce  $P$ . It also depends on the minimum time to produce one unit of  $P$   $\tau_P$ , and the minimum time to use resource  $R_j$  in order to produce one  $P$   $\tau_i$ . If resources are not fully allocated to the production of one product  $P$ , and several products  $P_i$  are assembled in parallel, one resource may be used by different production chains simultaneously. In this case a fraction  $\alpha_{i,j}$  of total available resources  $R_j$  must be used to produce  $P_i$ , so that

$$\frac{dP_i}{dt} = \frac{1}{\tau_P} \min \left( \alpha_{i,1} \frac{\tau_P R_1}{\tau_1 n_1}, \alpha_{i,2} \frac{\tau_P R_2}{\tau_2 n_2}, \dots, \alpha_{i,N} \frac{\tau_P R_N}{\tau_N n_N} \right). \quad (17)$$

where  $\alpha_{i,j} \tau_P / \tau_j n_j$  represents the maximal number of copies of the product that you can produce simultaneously from one unit of resource  $i$ . In our model,  $1/k_{B,1}$  (resp.  $1/k_{C,1}$ ) is the minimal time required to use  $B_{1,u}$  (resp.  $C_{1,u}$ ) in order to increase either  $B_2$  or  $C_2$ .

Within Leontief's approach [31], or Liebig's model in ecology [32], the rates of reactions involving two complementary resources are set by the limiting quantity among the two using a minimum function as shown in Fig. 1a. We use numbers rather than concentrations in order to use the law of the minimum of Leontief's formalism. In particular, for a number  $N$  of individuals in a volume  $\Omega$ , the concentration is  $c = N/\Omega$ . We get:

$$\frac{dc}{dt} = \frac{1}{\Omega} \frac{dN}{dt} - c \frac{1}{\Omega} \frac{d\Omega}{dt}, \quad (18)$$

where the second term is the so called "dilution term"  $-\lambda c$ , with the growth rate  $\lambda = (1/\Omega)(d\Omega/dt)$ . Therefore, if we assume steady states for the concentration  $c$ , we get:

$$\frac{dN}{dt} = \lambda N. \quad (19)$$

### A.1 Simplified model

Here, we consider the network shown on Fig.1, in which at most three intermediates are present for ribosomes or RNA precursors. We will later relax this assumption and consider an arbitrary number of intermediates:

$$\begin{aligned}
\frac{dB_{1,u}}{dt} &= k_{B3}B_3 - k_{B4}B_{1,u} - \hat{k}_{on}\frac{A}{\Omega}B_{1,u} + k_{off}B_{1,b} - \frac{B_{1,u}}{\tau_{life}} \\
\frac{dB_{1,b}}{dt} &= \hat{k}_{on}\frac{A}{\Omega}B_{1,u} - k_{off}B_{1,b} - \frac{B_{1,b}}{\tau_{life}} \\
\frac{dB_2}{dt} &= \min(k_{B1}B_{1,u}, k_{C1}C_1) - k_{B2}B_2 - \frac{B_2}{\tau_{life}} \\
\frac{dB_3}{dt} &= k_{B2}B_2 - k_{B3}B_3 + k_{B4}B_{1,u} - \frac{B_3}{\tau_{life}} \\
\frac{dC_1}{dt} &= k_{C3}C_3 - k_{C4}C_1 - \frac{C_1}{\tau_{life(C)}} \\
\frac{dC_2}{dt} &= \min(k_{B1}B_{1,u}, k_{C1}C_1) - k_{C2}C_2 - \frac{C_2}{\tau_{life(C)}} \\
\frac{dC_3}{dt} &= k_{C2}C_2 - k_{C3}C_3 + k_{C4}C_1 - \frac{C_3}{\tau_{life(C)}} \\
\frac{dA}{dt} &= \hat{P}_{in}a_{ex}\Omega - P_{out}A - \hat{k}_{on}\frac{A}{\Omega}B_{1,u} + k_{off}B_{1,b},
\end{aligned} \tag{20}$$

where  $k_i$  and  $\hat{k}_i$  are rate constants. We now introduce the ribosome concentration  $\rho$  such that  $\Omega = B_{tot}/\rho$ . This ribosome concentration is assumed to be a constant [52], which does not depend on the antibiotic concentration. Thus, we can absorb the factor  $\rho$  into  $k_{on}$  using  $k_{on} = \hat{k}_{on}\rho$  and similarly with  $P_{in} = \hat{P}_{in}/\rho$ . When the species  $B$  is limiting, the minimum function can be simplified, the equations for  $C_1$ ,  $C_2$  and  $C_3$  may be discarded and we get a simpler system:

$$\begin{aligned}
\frac{dB_{1,u}}{dt} &= k_{B3}B_3 - k_{B4}B_{1,u} - k_{on}\frac{A}{B_{tot}}B_{1,u} + k_{off}B_{1,b} - \frac{B_{1,u}}{\tau_{life}} \\
\frac{dB_{1,b}}{dt} &= k_{on}\frac{A}{B_{tot}}B_{1,u} - k_{off}B_{1,b} - \frac{B_{1,b}}{\tau_{life}} \\
\frac{dB_2}{dt} &= k_{B1}B_{1,u} - k_{B2}B_2 \\
\frac{dB_3}{dt} &= k_{B2}B_2 - k_{B3}B_3 + k_{B4}B_{1,u} - \frac{B_3}{\tau_{life}} \\
\frac{dA}{dt} &= P_{in}B_{tot}a_{ex} - P_{out}A - k_{on}\frac{A}{B_{tot}}B_{1,u} + k_{off}B_{1,b}.
\end{aligned} \tag{21}$$

Let now assume that this system has a largest eigenvalue  $\lambda$ , which describes exponential growth. Since we are interested in a regime of balanced growth, this factor  $\lambda$  also represents the dilution rate that follows from the growth of the cell volume. Let us then also assume that the life time of the ribosome precursors  $\tau_{life}$  is long with respect to  $1/\lambda$ . In that case we obtain the system

$$\begin{aligned}
& \left( \lambda + k_{on} \frac{A}{B_{tot}} + k_{B4} \right) B_{1,u} = k_{B3} B_3 + k_{off} B_{1,b} \\
& (\lambda + k_{off}) B_{1,b} = k_{on} \frac{A}{B_{tot}} B_{1,u} \\
& (\lambda + k_{B2}) B_2 = k_{B1} B_{1,u} \\
& (\lambda + k_{B3}) B_3 = k_{B2} B_2 + k_{B4} B_{1,u} \\
& \left( \lambda + P_{out} + k_{on} \frac{B_{1,u}}{B_{tot}} \right) A = P_{in} B_{tot} a_{ex} + k_{off} B_{1,b}.
\end{aligned} \tag{22}$$

We now normalize all quantities with respect to the total amount of mature  $B$  molecules,  $B_{tot} = B_{1,u} + B_{1,b} + B_3$ . We find by summing equations 1, 2 and 4 of the previous system:

$$\lambda (B_{1,u} + B_{1,b} + B_3) = k_{B2} B_2, \tag{23}$$

which is equivalent to  $\lambda B_{tot} = k_{B2} B_2$ .

From the other equations, we have (third equation of Eq.22 and definition of  $B_{tot}$ ):

$$\begin{aligned}
& (\lambda + k_{B2}) B_2 = k_{B1} B_{1,u} \\
& B_{1,b} = B_{tot} - B_{1,u} - B_3 = B_{tot} - B_{1,u} - \frac{k_{B2} B_2 + k_{B4} B_{1,u}}{\lambda + k_{B3}}.
\end{aligned} \tag{24}$$

From this, we recover the equivalent of the first growth law for ribosomes (combining Eq.23 and the first of Eq.24):

$$\frac{B_{1,u}}{B_{tot}} = \frac{\lambda}{k_{B1}} \left( 1 + \frac{\lambda}{k_{B2}} \right). \tag{25}$$

To simplify the calculations, we introduce the notation  $Q(\lambda) := B_{1,u}/B_{tot}$  in the following.

The other equations give

$$\begin{aligned}
& \frac{B_2}{B_{tot}} = \frac{\lambda}{k_{B2}}, \\
& \frac{B_{1,b}}{B_{tot}} = 1 - \frac{\lambda}{k_{B1}} \left( 1 + \frac{\lambda}{k_{B2}} \right) - \frac{\lambda}{\lambda + k_{B3}} - \frac{k_{B4} \lambda \left( 1 + \frac{\lambda}{k_{B2}} \right)}{k_{B1} (\lambda + k_{B3})}.
\end{aligned} \tag{26}$$

Using the second equation of Eq. 22, we can write  $B_{1,b}$  in another way:

$$B_{1,b} = \frac{k_{on} A B_{1,u}}{B_{tot} (\lambda + k_{off})} = \frac{k_{on} A Q(\lambda)}{\lambda + k_{off}}, \tag{27}$$

and compute explicitly the abundance of antibiotics from the last equation of Eq.22:

$$A = \frac{P_{in} B_{tot} a_{ex}}{\lambda + P_{out} + \frac{k_{on} \lambda Q(\lambda)}{\lambda + k_{off}}}. \tag{28}$$

Now we can eliminate  $A$  from the previous two equations, which leads to a new expression for  $B_{1,b}$ :

$$B_{1,b} = \frac{P_{in} a_{ex} B_{tot} k_{on} Q(\lambda)}{(\lambda + k_{off})(\lambda + P_{out}) + k_{on} Q(\lambda) \lambda}. \tag{29}$$

## A.2 Inhibitor-free growth rate

Without toxic agent ( $a_{ex} = 0$ ), we obtain from Eq.29  $B_{1,b} = 0$ , which implies using Eq.26 the equation

$$k_{B1}k_{B3} = \lambda_0 (\lambda_0 + k_{B3} + k_{B4}) \left(1 + \frac{\lambda_0}{k_{B2}}\right), \quad (30)$$

where,  $\lambda_0$  is the value of  $\lambda$  in the absence of inhibitor, i.e. the "inhibitor-free" growth rate of the cell. As the concentration of antibiotics increases, the growth rate is modified. In particular, we always have  $\lambda \leq \lambda_0$  for bacteriostatic drugs.

## A.3 Second growth law

To recover the second growth law, we simply sum Eq.25 and Eq.26:

$$\frac{B_{1,u} + B_{1,b}}{B_{tot}} = \frac{k_{B3} - k_{B4}Q(\lambda)}{\lambda + k_{B3}}. \quad (31)$$

In the limit of fast assembly ( $k_{B2}, k_{B3} \gg \lambda$ ), we find  $Q(\lambda) \simeq \lambda/k_{B1}$  and

$$\frac{B_{1,u} + B_{1,b}}{B_{tot}} = 1 - \frac{\lambda}{k_{B3}} \left(1 + \frac{k_{B4}}{k_{B1}}\right), \quad (32)$$

which assuming in addition fast activation ( $k_{B4} \ll k_{B1}$ ) further simplifies in

$$\frac{B_{1,u} + B_{1,b}}{B_{tot}} = 1 - \frac{\lambda}{k_{B3}}. \quad (33)$$

Note that this model always predicts a negative correlation between the growth rate and the ratio  $(B_{1,u} + B_{1,b})/B_{tot}$  if the growth rate is high enough from Eq. 31 because  $Q(\lambda)$  is a quadratic function of  $\lambda$ . In the limit of fast assembly ( $k_{B2}, k_{B3} \gg \lambda$ ), this correlation takes the form of a linear dependence in  $\lambda$  in agreement with [17].

## A.4 Self-consistent equation for the growth rate

Without any assumptions on the rates, equating the two equations for  $B_{1,b}$  (Eq.26 and Eq.29) yields the self-consistent equation for the growth rate:

$$\frac{P_{in}a_{ex}k_{on}Q(\lambda)}{(\lambda + P_{out})(\lambda + k_{off}) + k_{on}\lambda Q(\lambda)} = \frac{k_{B3} - (k_{B3} + k_{B4} + \lambda)Q(\lambda)}{\lambda + k_{B3}}. \quad (34)$$

In order to obtain a more manageable expression, we now assume:  $k_{B3} \gg k_{B4}$  and  $(k_{B2}, k_{B3} \gg \lambda_0)$ , which lead to  $\lambda_0 \simeq k_{B1}$  and  $Q(\lambda) \simeq \lambda/\lambda_0$ . These approximations are expected to hold for ribosomes which can be described by long lifetimes, fast assembly and fast activation rates. Since  $\lambda < \lambda_0$ , this approximation also implies  $(k_{B2}, k_{B3} \gg \lambda)$ , and therefore Eq. 34 takes the simpler form of a cubic equation for  $\lambda$ :

$$P_{in}a_{ex}k_{on}\frac{\lambda}{\lambda_0} = \left(1 - \frac{\lambda}{\lambda_0}\right) \left[ (\lambda + k_{off})(\lambda + P_{out}) + k_{on}\frac{\lambda^2}{\lambda_0} \right]. \quad (35)$$

### A.4.1 Reversible limit

Let us now introduce a typical growth rate  $\lambda_0^* = 2\sqrt{P_{out}K_D\lambda_0}$  where  $K_D = k_{off}/k_{on}$ . In the reversible limit defined by  $\lambda \ll \lambda_0^*$ , one also has  $P_{out}, k_{off} \gg \lambda$  and thus Eq. 35 leads to

$$\frac{\lambda}{\lambda_0} (K_D P_{out} + P_{in}a_{ex}) = K_D P_{out}, \quad (36)$$

and therefore:

$$\lambda = \frac{\lambda_0}{1 + \frac{P_{in}a_{ex}}{K_D P_{out}}}, \quad (37)$$

which is the result obtained in [13] for the reversible case.

#### A.4.2 Irreversible limit

In the irreversible limit instead,  $\lambda \gg \lambda_0^*$ . This implies  $P_{out}, k_{off} \ll \lambda$  and  $k_{on} \gg \lambda_0$ ,

545

546

$$\left(\frac{\lambda}{\lambda_0}\right)^2 - \left(\frac{\lambda}{\lambda_0}\right) + \frac{P_{in}a_{ex}}{\lambda_0} = 0. \quad (38)$$

In this case:

$$\lambda = \frac{\lambda_0}{2} \left(1 + \sqrt{1 - \frac{4P_{in}a_{ex}}{\lambda_0}}\right), \quad (39)$$

also in agreement with [13].

#### A.5 General case: arbitrary number of intermediate construction steps

For some processes (such as the autocatalytic cycle of RNA polymerase [18]), some intermediate steps can be significant to form mature autocatalysts  $B_1$  as sketched on Fig 1a of the main text. As an example, to form RNA-polymerase, mRNA have to be translated to resting protein subunits, that have to be activated and then assembled to form resting RNA-polymerase ( $B_{N-1}$  in Fig. 1a, with  $N = 5$  in this example).

551

552

553

554

555

556

557

558

559

560

561

562

Examples from ecology, or economy could involve slow assembly steps affecting the growth rate. Typically, if one sub-unit of the system is produced slowly we expect the system to be limited by this step, whereas fast assembly steps should not influence the growth rate. Here, we extend the previous model to include an arbitrary number of intermediate steps. Below, we do this for the first cycle only, assuming  $B$  is limiting as done previously.

The rate equations now become:

$$\begin{aligned} \frac{dB_{1,u}}{dt} &= k_{B,N}B_N - k_{B,N+1}B_{1,u} - k_{on}\frac{A}{B_{tot}}B_{1,u} + k_{off}B_{1,b} - \frac{B_{1,u}}{\tau_{life}} \\ \frac{dB_{1,b}}{dt} &= k_{on}\frac{A}{B_{tot}}B_{1,u} - k_{off}B_{1,b} - \frac{B_{1,b}}{\tau_{life}} \\ \frac{dB_2}{dt} &= k_{B,1}B_{1,u} - k_{B,2}B_2 \\ &\vdots \\ \frac{dB_N}{dt} &= k_{B,N-1}B_{N-1} - k_{B,N}B_N + k_{B,N+1}B_{1,u} - \frac{B_N}{\tau_{life}} \\ \frac{dA}{dt} &= P_{in}B_{tot}a_{ex} - P_{out}A - k_{on}\frac{A}{B_{tot}}B_{1,u} + k_{off}B_{1,u} \end{aligned} \quad (40)$$

With the assumption of exponential growth with a rate  $\lambda$  and that of a long life time  $1/\tau_{life} \ll \lambda$ , we obtain the system:

563

564

$$\begin{aligned}
& \left( \lambda + k_{B,N+1} + k_{on} \frac{A}{B_{tot}} \right) B_{1,u} = k_{B,N} B_N + k_{off} B_{1,b} \\
& (\lambda + k_{off}) B_{1,b} = k_{on} \frac{A}{B_{tot}} B_{1,u} \\
& (\lambda + k_{B,2}) B_2 = k_{B,1} B_{1,u} \\
& \vdots \\
& (\lambda + k_{B,N-1}) B_{N-1} = k_{B,N-2} B_{N-2} \\
& (\lambda + k_{B,N+}) B_N = k_{B,N-1} B_{N-1} + k_{B,N+1} B_{1,u} \\
& \left( \lambda + P_{out} + k_{on} \frac{B_{1,u}}{B_{tot}} \right) A = P_{in} B_{tot} a_{ex} + k_{off} B_{1,u},
\end{aligned} \tag{41}$$

and if we multiply equations 3 to  $N$  together, we find:

$$B_{1,u} = \frac{\lambda + k_{B,N-1}}{k_{B,1}} \left( 1 + \frac{\lambda}{k_{B,2}} \right) \times \dots \times \left( 1 + \frac{\lambda}{k_{B,N-2}} \right) B_{N-1}. \tag{42}$$

Defining  $B_{tot} = B_{1,u} + B_{1,b} + B_N$ , we obtain by summing the two first equations and the  $N+1$ -th:

$$B_{N-1} = \frac{\lambda}{k_{B,N-1}} B_{tot}, \tag{43}$$

and therefore, we get:

$$\frac{B_{1,u}}{B_{tot}} = \frac{\lambda}{k_{B,1}} \left( 1 + \frac{\lambda}{k_{B,2}} \right) \times \dots \times \left( 1 + \frac{\lambda}{k_{B,N-1}} \right). \tag{44}$$

This is the equivalent of the first growth law [13, 15, 18] in a general case, and in that case,  $B_{1,u}/B_{tot}$  is a  $(N-1)$ -th order polynomial in  $\lambda$ , which we call  $Q(\lambda)$ . This polynomial is positive and increasing over  $\mathbb{R}^+$ . Now, if all the intermediate processes are sufficiently fast  $\forall n \in \{2, \dots, N-1\}, \lambda \ll k_{B,n}$ , we recover the linear law:

$$B_{1,u} = \frac{\lambda}{k_{B,1}} B_{tot}. \tag{45}$$

We can also express the concentration of bound individuals  $B_{1,b}$ :

$$\frac{B_{1,b}}{B_{tot}} = \frac{k_{B,N} - Q(\lambda)(\lambda + k_{B,N} + k_{B,N+1})}{\lambda + k_{B,N}}, \tag{46}$$

we further obtain:

$$\begin{aligned}
B_{1,u} &= Q(\lambda) B_{tot} \\
B_{1,b} &= \frac{k_{B,N} - Q(\lambda)(\lambda + k_{B,N} + k_{B,N+1})}{\lambda + k_{B,N}} B_{tot} \\
B_{1,b} &= \frac{k_{on} A Q(\lambda)}{\lambda + k_{off}} \\
A &= \frac{P_{in} B_{tot} a_{ex}}{\lambda + P_{out} + k_{on} Q(\lambda) \frac{\lambda}{\lambda + k_{off}}}.
\end{aligned} \tag{47}$$

The second equation is obtained by writing  $B_{1,b} = B_{tot} - B_{1,u} - B_N$ . Equating the two equations for  $B_{1,b}$ , we find the general self-consistent equation on the growth rate Eq.49. In the absence of toxic agent,  $a_{ex} = 0$ , the growth rate  $\lambda_0$  is set by:

$$Q(\lambda_0)(\lambda_0 + k_{B,N} + k_{B,N+1}) = k_{B,N}. \quad (48)$$

As done previously, we can write a second expression for  $B_{1,b}$  as proportional to the abundance of toxic agents  $A$ . Equating the two equations for  $B_{1,b}$ , we find a general self-consistent equation on the growth rate, which becomes equivalent to Eq. 3 of the main text when there is only one assembly step ( $N = 3$ ):

$$\frac{k_{on}Q(\lambda)P_{in}a_{ex}(\lambda + k_{B,N})}{(\lambda + k_{off})(\lambda + P_{out} + k_{on}Q(\lambda)\frac{\lambda}{\lambda + k_{off}})} = k_{B,N} - Q(\lambda)(\lambda + k_{B,N} + k_{B,N+1}). \quad (49)$$

In the absence of toxic agent,  $a_{ex} = 0$ , and the growth rate  $\lambda_0$  is set by taking the right side of the equation to be 0. This is a generalization of the results discussed previously in the simple case, and we can generalize our results from this new set of equations. In particular we can add several limiting steps (with slow rates), in which case the behaviour of the growth rate with antibiotic concentration is smoothed.

## B Experimental data and fitting procedure

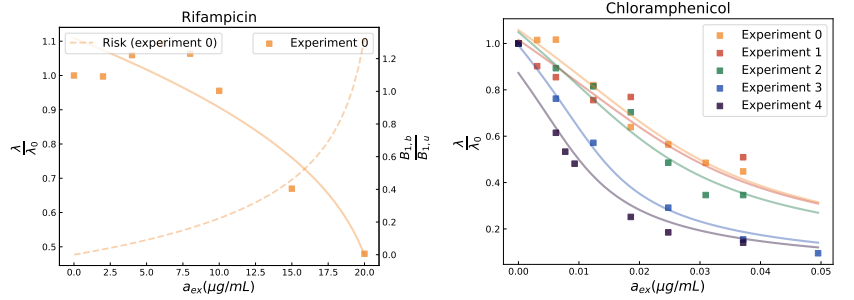
### B.1 List of compounds analyzed in this work

Chloramphenicol (Fig.8b) inhibits ribosome production by binding to ribosomes (preventing them from transcribing new proteins). Its effect on growth laws has been studied [13] as an example of bacteriostatic drug on E.Coli. Rifampicin (Fig.8a) targets RNA-polymerase by binding to RNA-polymerase [38, 39](thus inhibiting the RNA-polymerase autocatalytic cycle discussed in [18]). With our formalism, we also describe the effect of Triclosan (Fig.8c), Erythromycin (Fig.8d), Streptomycin (Fig.8e) and Kanamycin (Fig.8f), which have different modes of action but are all bacteriostatic drugs against E.Coli. Kanamycin, Streptomycin, Chloramphenicol and Erythromycin target the ribosomal autocatalytic cycle at different stages and inhibit growth [4, 6, 8, 40]. Triclosan acts as a bacteriostatic by targeting the synthesis of fatty acids [41–43], and thus affecting the building of bacterial membranes [18].

### B.2 Fitting procedure for the various antibiotics

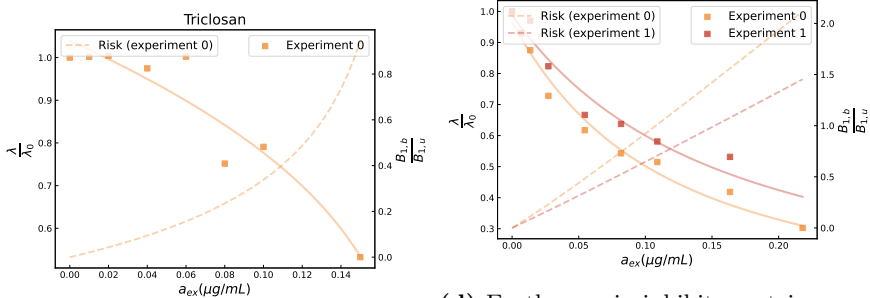
In order to recover the growth rate dependencies on drug concentration of Fig.8, we fitted our expression Eq.49 with different sets of data, where  $Q(\lambda)$  is given by Eq.44.

We consider  $N = 6$  and separate the  $N$  processes between fast and slow intermediary steps. For all antibiotics we assume that there is one no limiting step, to use the results of the main text. The steps are fast, and  $(k_{B,n})_{2 \leq n \leq 6}$  are set to  $10^5 h^{-1}$  (arbitrary high value compared to  $\lambda$ , in order to neglect those steps) so that  $\lambda/k_{B,n} \ll 1$  for  $n \geq 2$ . For a given antibiotic, different experiments correspond to different growth conditions ([9, 13]), that may affect the parameters of the model. As the number of free parameters is high, we constrained them in order to have biologically accurate values. From [9, 13, 54], we expect the basal growth rate  $\lambda_0$  to be of order  $1 h^{-1}$  (as measured in [13]). The binding and unbinding rates, and the influx and outflux are expected to be



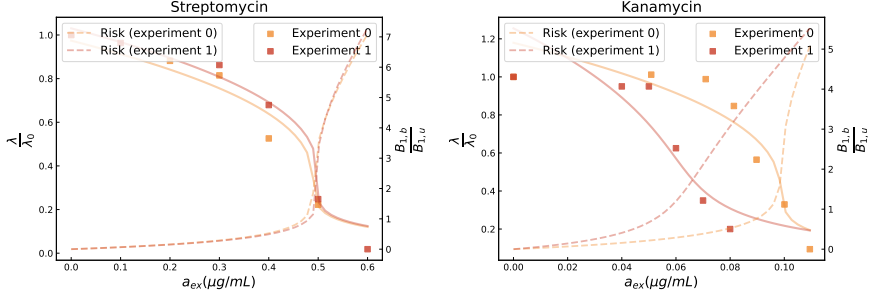
(a) Rifampicin targets RNA-polymerase and inhibits RNA synthesis [38]. Data from [9].

(b) Chloramphenicol inhibits protein synthesis by binding to ribosomes [5]. Data from [9].



(c) Triclosan targets the synthesis of fatty acids [41]. Data from [9].

(d) Erythromycin inhibits protein synthesis by binding to ribosomal proteins [53]. Data from [9].



(e) Streptomycin inhibits protein synthesis by binding to ribosomal proteins [13]. Data from [13].

(f) Kanamycin inhibits protein synthesis by binding to ribosomal proteins [13]. Data from [13].

**Fig 8.** Comparison with experiments for various drugs. In solid lines, we show the growth rate as a function of the fraction of inhibitors. In dotted lines, we show a measure of the risk  $\frac{B_{1,b}}{B_{1,u}}$ . This measure compares the abundance of bound individuals  $B_{1,b}$  to that of unbound operational individuals  $B_{1,u}$  as in Eq 14. For ribosome-targeting drugs, this corresponds to the fraction of bound ribosomes (inhibited) to unbound ribosomes (operating). Unbound ribosomes are indeed required for the vital functions of the cell whereas bound ribosomes are unable to synthesize proteins.

	$P_{in}(mL \cdot \mu g^{-1} \cdot h^{-1})$	$P_{out}(h^{-1})$	$k_{B,1}(h^{-1})$	$k_{B,N+1}(h^{-1})$	Experimental growth conditions
Triclosan	2.85	4.33	1.28	$1. \times 10^{-3}$	MOPS glucose + 6 a. a.
Chloramphenicol (0)	55.4	44.4	1.87	0.1	TSB (Tryptic soy broth)
Chloramphenicol (1)	53.6	44.4	1.78	0.1	TSB (Tryptic soy broth)
Chloramphenicol (2)	53.6	37.56	1.52	0.1	MOPS glucose synthetic rich
Chloramphenicol (3)	80.4	29.6	1.66	$1. \times 10^{-3}$	Rich MOPS (0.2% glucose)
Chloramphenicol (4)	80.4	29.6	1.18	$1. \times 10^{-3}$	Rich MOPS (0.2% glycerol)
Rifampicin	$2.20 \times 10^{-2}$	3.46	1.32	$1.0 \times 10^{-3}$	MOPS glucose + 6 a. a.
Erythromycin (0)	$1.87 \times 10^2$	$8.9 \times 10^2$	1.16	$1.0 \times 10^{-3}$	MOPS glucose + 6 a. a.
Erythromycin (1)	$1.35 \times 10^2$	$9.6 \times 10^2$	$6.35 \times 10^{-1}$	$1. \times 10^{-1}$	MOPS glycerol
Streptomycin (0)	0.77	2.4	1.04	0.1	Rich MOPS (0.2% glycerol)
Streptomycin (1)	0.69	1.85	1.12	$9.9 \times 10^{-2}$	MOPS (0.2% glucose, 0.2% casamino acids)
Kanamycin (0)	3.60	1.97	1.16	$8.0 \times 10^{-3}$	MOPS (0.2% glycerol, 0.2% casamino acids)
Kanamycin (1)	4.73	1.85	1.09	$3.8 \times 10^{-3}$	MOPS medium (0.2% glycerol)

**Table 2.** Parameters estimated from the fitting procedure (using the package `scipy.optimize`)

faster, typically ranging between  $1h^{-1}$  and  $1000h^{-1}$  [13, 14, 55]. From this considerations, we allow  $k_{B,1}$  to vary between  $0.4h^{-1}$  and  $4h^{-1}$ ,  $P_{out}$  to vary between  $0h^{-1}$  and  $10^3h^{-1}$  and  $P_{in}$  to vary between  $0\mu g.mL^{-1}.h^{-1}$  and  $10^3\mu g.mL^{-1}.h^{-1}$  to capture the effects of reversibility. To reduce the number of free parameters, we set  $K_D = k_{off}/k_{on} = 1/50$  and  $k_{off} = 5h^{-1}$ . And the deactivation rate  $k_{B,N+1} \in [10^{-3}h^{-1}; 10^{-1}h^{-1}]$  is typically small compared to  $\lambda$ . From a biological point of view, as the different experiments used for one antibiotic correspond to various growth medium, we can consider that the reaction rates may vary from one experiment to the next, but we can assume that for a given antibiotic  $P_{in}$  and  $P_{out}$  weakly vary. By adding this constraint, there are 4 parameters for each antibiotic but  $P_{in}$  and  $P_{out}$  cannot vary more than 20% for different growth medium and a given antibiotic. In order to use concentrations in  $\mu g/mL$  from the data in  $\mu M$  for Chloramphenicol and Erythromycin we use molar masses (323.132g/mol for Chloramphenicol and 733.93g/mol for Erythromycin).

## C Complements

### C.1 Combined effect of two antibiotics targeting different cycles

In order to produce Fig.6 of the main text, we solve the system for coupled autocatalytic cycles with two antibiotics obtained by keeping the min function in Eq.20 and using exponential solution (with the growth rate  $\lambda$ )

$$\begin{aligned}
\lambda + \frac{1}{\tau_{life}} &= \frac{k_{B,2}}{\lambda + k_{B,2} + \frac{1}{\tau_{life(B)}}} \min(k_{B,1} \frac{B_{1,u}}{B_{tot}}, k_{C,1} \frac{C_{1,u}}{B_{tot}}) \\
\lambda + \frac{1}{\tau_{life(C)}} &= \frac{k_{C,2}}{\lambda + k_{C,2} + \frac{1}{\tau_{life}} \frac{1}{\tau_{life(C)}}} \min(k_{B,1} \frac{B_{1,u}}{C_{tot}}, k_{C,1} \frac{C_{1,u}}{C_{tot}}) \\
\frac{B_{1,b}}{B_{tot}} &= \frac{k_{on(B)} A_1}{\lambda + k_{off(B)} + \frac{1}{\tau_{life(B)}}} \frac{B_{1,u}}{B_{tot}} \\
\frac{C_{1,b}}{C_{tot}} &= \frac{k_{on(C)} A_2}{\lambda + k_{off(C)} + \frac{1}{\tau_{life(C)}}} \frac{C_{1,u}}{C_{tot}} \\
1 - \frac{B_{1,u}}{B_{tot}} - \frac{B_{1,b}}{B_{tot}} &= \frac{k_{B,2}}{(\lambda + k_{B,2} + \frac{1}{\tau_{life(B)}})(\lambda + k_{B,3} + \frac{1}{\tau_{life(B)}})} \min(k_{B,1} \frac{B_{1,u}}{B_{tot}}, k_{C,1} \frac{C_{1,u}}{B_{tot}}) \\
1 - \frac{C_{1,u}}{C_{tot}} - \frac{C_{1,b}}{C_{tot}} &= \frac{k_{C,2}}{(\lambda + k_{C,2} + \frac{1}{\tau_{life(C)}})(\lambda + k_{C,3} + \frac{1}{\tau_{life(C)}})} \min(k_{B,1} \frac{B_{1,u}}{C_{tot}}, k_{C,1} \frac{C_{1,u}}{C_{tot}}) \\
\frac{A_1}{B_{tot}} &= \frac{1}{\lambda + P_{out(B)} + k_{on} \frac{B_{1,u}}{B_{tot}}} \left( P_{in(B)} a_{ex,1} + k_{off} \frac{B_{1,b}}{B_{tot}} \right) \\
\frac{A_2}{C_{tot}} &= \frac{1}{\lambda + P_{out(C)} + k_{on} \frac{C_{1,u}}{C_{tot}}} \left( P_{in(C)} a_{ex,2} + k_{off} \frac{C_{1,b}}{C_{tot}} \right).
\end{aligned}$$

The two first equations correspond to summing the equations for  $B_{1,u}$ ,  $B_{1,b}$  and  $B_3$  (resp. for  $C_{1,u}$ ,  $C_{1,b}$  and  $C_3$ ). The third and fourth equations are obtained from the equations on  $B_{1,b}$  (resp.  $C_{1,b}$ ). The fifth and sixth equations result from the equation on  $B_2$  replaced in the equation for  $B_3$ . Finally, the two last equations follow from the equations  $A_1$  and  $A_2$ .

**Example with one building step in each cycle, one irreversible cycle and one reversible cycle** If the first cycle is reversible, we have on one hand

$$\lambda = \frac{k_{B,1}}{1 + \frac{K_{D(B)} P_{in(B)}}{P_{out(B)}} a_{ex,1}}, \quad (51)$$

and on the other hand, as the second cycle is irreversible

$$\lambda = \frac{k_{C,1}}{2} \left( 1 + \sqrt{1 - \frac{4P_{in(C)} a_{ex,2}}{k_{C,1}}} \right). \quad (52)$$

For small concentrations of both antibiotics, we get a linear transition, which we observe on Fig.6 of the main text

$$a_{ex,2} = \frac{k_{B,1} K_{D(B)} P_{in(B)}}{P_{in(C)} P_{out(B)}} a_{ex,1} + \frac{k_{C,1} - k_{B,1}}{P_{in(C)}}, \quad (53)$$

which simplifies into  $a_{ex,2} = k_{B,1} a_{ex,1} K_{D(B)} / P_{out(B)}$  when the drugs have the same parameters for  $P_{in}$  and  $k_{B,1}$ .

**Example with one building step in each cycle, both reversible** With two reversible cycles, for small concentrations of both antibiotics, in the particular case that both drugs have the same parameters, the transition occurs at  $a_{ex,1} = a_{ex,2}$ , which is observed on Fig.6 of the main text.

## C.2 Consequences of the inhibition of the first cycle on the second cycle

To understand the effect of the  $B$  cycle on the other one, the  $C$  cycle in Fig.1 of the main text, we still assume  $B$  species limiting, so the minimum function between  $B_{1u}$  and  $C_1$  in the equation for the production of  $C_2$  gives  $B_{1u}$ . Now we focus on the equations for the  $C$  species. Assuming again exponential growth with the same growth rate  $\lambda$  in both cycles, we show the effect on  $C_1$  on Fig.9. The increase in the relative amount  $C_1/B_{tot}$  for intermediate values is only observed for  $\tau_{life(C)} < \tau_{life(B)}$  and correspond to an accumulation of  $C$  at long time. We recover the distinction between the reversible and irreversible cases. We also observe that there are regimes where  $C_1$  increases with  $a_{ex}$ , which are obtained for  $\tau_{life(C)} < \tau_{life(B)}$ . Assuming again exponential growth with the same growth rate  $\lambda$  in both cycles, we get:

$$\begin{aligned} \left( \lambda + \frac{1}{\tau_{life(C)}} \right) C_1 &= k_{C3} C_3 - k_{C4} C_1 \\ (\lambda + k_{C2}) C_2 &= k_{B1} B_{1u} \\ \left( \lambda + \frac{1}{\tau_{life(C)}} + k_{C3} \right) C_3 &= k_{C4} C_1 + k_{C2} C_2. \end{aligned} \quad (54)$$

Now if we introduce the total abundance of  $C$ ,  $C_{tot} = C_1 + C_3$ :

$$\begin{aligned} \left( \lambda + \frac{1}{\tau_{life(C)}} \right) C_{tot} &= k_{C2} C_2 \\ (\lambda + k_{C2}) C_2 &= k_{B1} Q(\lambda) B_{tot} \\ \left( \lambda + \frac{1}{\tau_{life(C)}} + k_{C3} \right) C_{tot} &= \left( \lambda + \frac{1}{\tau_{life(C)}} + k_{C3} + k_{C4} \right) C_1 + k_{C2} C_2. \end{aligned} \quad (55)$$

We can express everything in terms of  $B_{tot}$ :

$$\begin{aligned} C_{tot} &= \frac{k_{B1} Q(\lambda)}{\left( \lambda + \frac{1}{\tau_{life(C)}} \right) \left( 1 + \frac{\lambda}{k_{C2}} \right)} B_{tot}, \\ C_2 &= \frac{k_{B1} Q(\lambda)}{\lambda + k_{C2}} B_{tot}, \\ C_1 &= \frac{k_{C3}}{\lambda + \frac{1}{\tau_{life(C)}} + k_{C3} + k_{C4}} \frac{k_{B1} Q(\lambda)}{\left( \lambda + \frac{1}{\tau_{life(C)}} \right) \left( 1 + \frac{\lambda}{k_{C2}} \right)} B_{tot}. \end{aligned} \quad (56)$$

From this we see that the second cycle is affected by the toxic agent via the growth rate. Note that here the difference in lifetimes matters, because as  $\lambda \rightarrow 0$ , we get (fast activation)

$$\frac{C_1}{B_{tot}} \sim \frac{k_{C3}}{\frac{1}{\tau_{life(C)}} + k_{C3} + k_{C4}} \frac{\tau_{life(C)}}{\tau_{life(B)}} \sim \frac{\tau_{life(C)}}{\tau_{life(B)}}. \quad (57)$$

In addition, we observe that for small enough values of  $a_{ex}$ , the relative abundance of  $C_1$  increases with  $a_{ex}$ . In this case, the slowing down of the first cycle does not affect strongly the second cycle. For large concentrations of antibiotics, the first cycle is frustrated and the second one becomes limited by the need for autocatalysts of type  $B$ , thus leading to lower relative abundances of  $C_1$ .

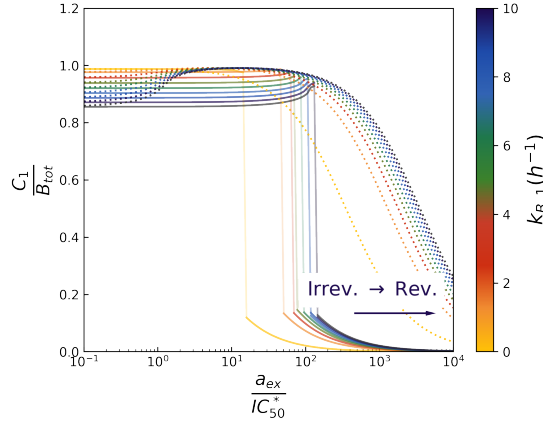


**Fig 9.** Fraction of autocatalysts in the second cycle when the first cycle is targeted by inhibitors.

### C.3 Closed compartment and inhibiting waste

For a closed compartment  $P_{in} = P_{out} = 0$  and waste  $W$  produced at rate  $k_w$ , the equations are

$$\begin{aligned} \left( \lambda + k_{on} \frac{W}{B_{tot}} + k_{B4} + k_w \right) B_{1,u} &= k_{B3} B_3 + k_{off} B_{1,b} \\ (\lambda + k_{off}) B_{1,b} &= k_{on} \frac{W}{B_{tot}} B_{1,u} \\ (\lambda + k_{B2}) B_2 &= k_{B1} B_{1,u} \\ (\lambda + k_{B3}) B_3 &= k_{B2} B_2 + k_{B4} B_{1,u} \\ \left( \lambda + k_{on} \frac{B_{1,u}}{B_{tot}} \right) W &= k_{off} B_{1,b} + k_w B_{1,u}. \end{aligned} \quad (58)$$

Therefore, we can express  $W/B_{tot}$  as a function of  $Q(\lambda)$  and replace it in the second equation to find the risk

$$\frac{B_{1,b}}{B_{1,u}} = \frac{k_{on} k_w Q(\lambda)}{(\lambda + k_{off}) \left( \lambda + k_{on} Q(\lambda) \frac{\lambda}{\lambda + k_{off}} \right)}. \quad (59)$$

## References

1. Davies J DD. Origins and Evolution of Antibiotic Resistance. *Microbiology and Molecular Biology Reviews*. 2010;(74). doi:<https://doi.org/10.1128/mmbr.00016-10>.
2. Chait R, Craney A, Kishony R. Antibiotic interactions that select against resistance. *Nature*. 2007;446(7136):668–671. doi:10.1038/nature05685.
3. Loree J, Lappin SL. Bacteriostatic Antibiotics. StatPearls Publishing, Treasure Island (FL); 2023. Available from: <http://europepmc.org/abstract/MED/31613458>.
4. Lin J, Zhou D, Steitz TA, Polikanov YS, Gagnon MG. Ribosome-Targeting Antibiotics: Modes of Action, Mechanisms of Resistance, and Implications for

- Drug Design. Annual review of biochemistry. 2018;87:451–478. doi:10.1146/annurev-biochem-062917-011942. 685  
686
5. Contreras A, Barbacid M, Vazquez D. Binding to ribosomes and mode of action of chloramphenicol analogues. Biochimica et Biophysica Acta (BBA) - Nucleic Acids and Protein Synthesis. 1974;349(3):376–388. doi:10.1016/0005-2787(74)90124-5. 687  
688  
689  
690
6. Mondal S, Pathak BK, Ray S, Barat C. Impact of P-Site tRNA and Antibiotics on Ribosome Mediated Protein Folding: Studies Using the Escherichia coli Ribosome. PLOS ONE. 2014;9(7):e101293. doi:10.1371/journal.pone.0101293. 691  
692  
693
7. Mosaei H, Harbottle J. Mechanisms of antibiotics inhibiting bacterial RNA polymerase. Biochemical Society Transactions. 2019;47(1):339–350. doi:10.1042/BST20180499. 694  
695  
696
8. Kohanski MA, Dwyer DJ, Wierzbowski J, Cottarel G, Collins JJ. Mistranslation of Membrane Proteins and Two-Component System Activation Trigger Antibiotic-Mediated Cell Death. Cell. 2008;135(4):679–690. doi:10.1016/j.cell.2008.09.038. 697  
698  
699  
700
9. Si F, Li D, Cox SE, Sauls JT, Azizi O, Sou C, et al. Invariance of Initiation Mass and Predictability of Cell Size in Escherichia coli. Current Biology. 2017;27(9):1278–1287. doi:10.1016/j.cub.2017.03.022. 701  
702  
703
10. Levin BR, McCall IC, Perrot V, Weiss H, Ovesepian A, Baquero F. A Numbers Game: Ribosome Densities, Bacterial Growth, and Antibiotic-Mediated Stasis and Death. mBio. 2017;8(1). doi:10.1128/mBio.02253-16. 704  
705  
706
11. Tuomanen E, Cozens R, Tosch W, Zak O, Tomasz A. The rate of killing of Escherichia coli by beta-lactam antibiotics is strictly proportional to the rate of bacterial growth. Journal of general microbiology. 1986;132(5):1297–1304. doi:10.1099/00221287-132-5-1297. 707  
708  
709  
710
12. Lopatkin AJ, Stokes JM, Zheng EJ, Yang JH, Takahashi MK, You L, et al. Bacterial metabolic state more accurately predicts antibiotic lethality than growth rate. Nature Microbiology. 2019;4(12):2109–2117. doi:10.1038/s41564-019-0536-0. 711  
712  
713
13. Greulich P, Scott M, Evans MR, Allen RJ. Growth-dependent bacterial susceptibility to ribosome-targeting antibiotics. Molecular systems biology. 2015;11(3):796. doi:10.15252/msb.20145949. 714  
715  
716
14. Svetlov MS, Vázquez-Laslop N, Mankin AS. Kinetics of drug–ribosome interactions defines the cidalty of macrolide antibiotics. Proceedings of the National Academy of Sciences. 2017;114(52):13673–13678. doi:10.1073/pnas.1717168115. 717  
718  
719  
720
15. Scott M, Hwa T. Bacterial growth laws and their applications. Nanobiotechnology and Systems Biology. 2011;22(4):559–565. doi:10.1016/j.copbio.2011.04.014. 721  
722
16. Wu C, Balakrishnan R, Braniff N, Mori M, Manzanarez G, Zhang Z, et al. Cellular perception of growth rate and the mechanistic origin of bacterial growth law. Proceedings of the National Academy of Sciences. 2022;119(20):e2201585119. doi:10.1073/pnas.2201585119. 723  
724  
725  
726
17. Scott M, Gunderson CW, Mateescu EM, Zhang Z, Hwa T. Interdependence of Cell Growth and Gene Expression: Origins and Consequences. Science. 2010;330(6007):1099–1102. doi:10.1126/science.1192588. 727  
728  
729

18. Roy A, Goberman D, Pugatch R. A unifying autocatalytic network-based framework for bacterial growth laws. *Proceedings of the National Academy of Sciences*. 2021;118(33):e2107829118. doi:10.1073/pnas.2107829118. 730  
731  
732
19. Lacoste D, Ledoux B. Universal features of autocatalytic systems. *Economic principles in cell biology*. 2025;. 733  
734
20. Chure G, Cremer J. An optimal regulation of fluxes dictates microbial growth in and out of steady state. *eLife*. 2023;12:e84878. doi:10.7554/eLife.84878. 735  
736
21. Calabrese L, Ciandrini L, Cosentino Lagomarsino M. How total mRNA influences cell growth. *Proceedings of the National Academy of Sciences*. 2024;121(21):e2400679121. doi:10.1073/pnas.2400679121. 737  
738  
739
22. Deris JB, Kim M, Zhang Z, Okano H, Hermsen R, Groisman A, et al. The Innate Growth Bistability and Fitness Landscapes of Antibiotic-Resistant Bacteria. *Science*. 2013;342(6162):1237435. doi:10.1126/science.1237435. 740  
741  
742
23. Kals M, Kals E, Kotar J, Donald A, Mancini L, Cicuta P. Antibiotics change the population growth rate heterogeneity and morphology of bacteria. *PLOS Pathogens*. 2025;21(2):e1012924. doi:10.1371/journal.ppat.1012924. 743  
744  
745
24. Allen R, Waclaw B. Antibiotic resistance: a physicist's view. *Phys Biol*. 2016;13(4):045001. 746  
747
25. Kavčič B, Tkačik G, Bollenbach T. Minimal biophysical model of combined antibiotic action. *PLOS Computational Biology*. 2021;17(1):e1008529. doi:10.1371/journal.pcbi.1008529. 748  
749  
750
26. Kavčič B, Tkačik G, Bollenbach T. Mechanisms of drug interactions between translation-inhibiting antibiotics. *Nat Commun*. 2020;11(1):4013. 751  
752
27. Bollenbach T, Quan S, Chait R, Kishony R. Nonoptimal Microbial Response to Antibiotics Underlies Suppressive Drug Interactions. *Cell*. 2009;139(4):707–718. doi:10.1016/j.cell.2009.10.025. 753  
754  
755
28. Chopra I. Molecular mechanisms involved in the transport of antibiotics into bacteria. *Parasitology*. 1988;96(S1):S25–S44. doi:10.1017/S0031182000085966. 756  
757
29. MacNair CR, Tan MW. The role of bacterial membrane vesicles in antibiotic resistance. *Annals of the New York Academy of Sciences*. 2023;1519(1):63–73. doi:10.1111/nyas.14932. 758  
759  
760
30. Yamagishi JF, Hatakeyama TS. Microeconomics of Metabolism: The Warburg Effect as Giffen Behaviour. *Bulletin of mathematical biology*. 2021;83(12):120. doi:10.1007/s11538-021-00952-x. 761  
762  
763
31. Dobos I, Floriska A. A Dynamic Leontief Model with Non-renewable Resources. *Economic Systems Research*. 2005;17(3):317–326. doi:10.1080/09535310500221856. 764  
765  
766
32. O'Neill RV, DeAngelis DL, Pastor JJ, Jackson BJ, Post WM. Multiple nutrient limitations in ecological models. *Ecological Modelling*. 1989;46(3):147–163. doi:10.1016/0304-3800(89)90015-X. 767  
768  
769
33. Pandey PP, Jain S. Analytic derivation of bacterial growth laws from a simple model of intracellular chemical dynamics. *Theory in Biosciences*. 2016;135(3):121–130. doi:10.1007/s12064-016-0227-9. 770  
771  
772

34. Thomas P, Terradot G, Danos V, Weiße AY. Sources, propagation and consequences of stochasticity in cellular growth. *Nature Communications*. 2018;9(1):4528. doi:10.1038/s41467-018-06912-9. 773  
774  
775
35. Elf J, Nilsson K, Tenson T, Ehrenberg M. Bistable Bacterial Growth Rate in Response to Antibiotics with Low Membrane Permeability. *Physical Review Letters*. 2006;97(25):258104. doi:10.1103/PhysRevLett.97.258104. 776  
777  
778
36. Irwin PL, Nguyen LHT, Paoli GC, Chen CY. Evidence for a bimodal distribution of Escherichia coli doubling times below a threshold initial cell concentration. *BMC Microbiology*. 2010;10(1):207. doi:10.1186/1471-2180-10-207. 779  
780  
781
37. Schultz D, Palmer AC, Kishony R. Regulatory Dynamics Determine Cell Fate following Abrupt Antibiotic Exposure. *Cell systems*. 2017;5(5):509–517.e3. doi:10.1016/j.cels.2017.10.002. 782  
783  
784
38. McClure WR, Cech CL. On the mechanism of rifampicin inhibition of RNA synthesis. *Journal of Biological Chemistry*. 1978;253(24):8949–8956. doi:10.1016/S0021-9258(17)34269-2. 785  
786  
787
39. Campbell EA, Korzheva N, Mustaev A, Murakami K, Nair S, Goldfarb A, et al. Structural Mechanism for Rifampicin Inhibition of Bacterial RNA Polymerase. *Cell*. 2001;104(6):901–912. doi:10.1016/S0092-8674(01)00286-0. 788  
789  
790
40. Chaturvedi SK, Siddiqi MK, Alam P, Khan RH. Protein misfolding and aggregation: Mechanism, factors and detection. *Process Biochemistry*. 2016;51(9):1183–1192. doi:10.1016/j.procbio.2016.05.015. 791  
792  
793
41. Heath RJ, Rubin JR, Holland DR, Zhang E, Snow ME, Rock CO. Mechanism of Triclosan Inhibition of Bacterial Fatty Acid Synthesis\*. *Journal of Biological Chemistry*. 1999;274(16):11110–11114. doi:10.1074/jbc.274.16.11110. 794  
795  
796
42. McMurry LM, Oethinger M, Levy SB. Triclosan targets lipid synthesis. *Nature*. 1998;394(6693):531–532. doi:10.1038/28970. 797  
798
43. Escalada MG, Harwood JL, Maillard JY, Ochs D. Triclosan inhibition of fatty acid synthesis and its effect on growth of Escherichia coli and Pseudomonas aeruginosa. *Journal of Antimicrobial Chemotherapy*. 2005;55(6):879–882. doi:10.1093/jac/dki123. 799  
800  
801  
802
44. Baquero F, Levin BR. Proximate and ultimate causes of the bactericidal action of antibiotics. *Nature Reviews Microbiology*. 2021;19(2):123–132. doi:10.1038/s41579-020-00443-1. 803  
804  
805
45. Himeoka Y, Horiguchi SA, Kobayashi TJ. Theoretical basis for cell deaths. *Physical Review Research*. 2024;6(4):043217. doi:10.1103/PhysRevResearch.6.043217. 806  
807  
808
46. Kiviet DJ, Nghe P, Walker N, Boulineau S, Sunderlikova V, Tans SJ. Stochasticity of metabolism and growth at the single-cell level. *Nature*. 2014;514(7522):376–379. doi:10.1038/nature13582. 809  
810  
811
47. Wada A, Igarashi K, Yoshimura S, Aimoto S, Ishihama A. Ribosome Modulation Factor: Stationary Growth Phase-Specific Inhibitor of Ribosome Functions from Escherichia coli. *Biochemical and Biophysical Research Communications*. 1995;214(2):410–417. doi:10.1006/bbrc.1995.2302. 812  
813  
814  
815

48. Zentou H, Zainal Abidin Z, Yunus R, Awang Biak DR, Abdullah Issa M, Yahaya Pudza M. A New Model of Alcoholic Fermentation under a Byproduct Inhibitory Effect. *ACS Omega*. 2021;6(6):4137–4146. doi:10.1021/acsomega.0c04025. 816  
817  
818  
819
49. Marrec L, Bitbol AF. Resist or perish: Fate of a microbial population subjected to a periodic presence of antimicrobial. *PLOS Computational Biology*. 2020;16(4):e1007798. doi:10.1371/journal.pcbi.1007798. 820  
821  
822
50. Le Quellec L, Aristov A, Gutiérrez Ramos S, Amselem G, Bos J, Baharoglu Z, et al. Measuring single-cell susceptibility to antibiotics within monoclonal bacterial populations. *PLOS ONE*. 2024;19(8):e0303630. doi:10.1371/journal.pone.0303630. 823  
824  
825  
826
51. Veldhuis MP, Berg MP, Loreau M, Olff H. Ecological autocatalysis: a central principle in ecosystem organization? *Ecological Monographs*. 2018;88(3):304–319. doi:10.1002/ecm.1292. 827  
828  
829
52. Neurohr GE, Amon A. Relevance and Regulation of Cell Density. *Trends in Cell Biology*. 2020;30(3):213–225. doi:10.1016/j.tcb.2019.12.006. 830  
831
53. Mazzei T, Mini E, Novelli A, Periti P. Chemistry and mode of action of macrolides. *Journal of Antimicrobial Chemotherapy*. 1993;31(suppl\_C):1–9. doi:10.1093/jac. 832  
833  
834
54. Koch Arthur L , Gross Gayle H . Growth Conditions and Rifampin Susceptibility. *Antimicrobial Agents and Chemotherapy*. 1979;15(2):220–228. doi:10.1128/aac.15.2.220. 835  
836  
837
55. Comby S, Flandrois JP, Carret G, Pichat C. Mathematical modelling of growth of *Escherichia coli* at subinhibitory levels of chloramphenicol or tetracyclines. *Research in Microbiology*. 1989;140(3):243–254. doi:10.1016/0923-2508(89)90079-X. 838  
839  
840  
841